International Journal of Modelling and Simulation

ISSN: (Print) (Online) Journal homepage: www.tandfonline.com/journals/tjms20

Mathematical analysis of a novel fractional order vaccination model for Tuberculosis incorporating susceptible class with underlying ailment

A. El-Mesady, Olumuyiwa James Peter, Andrew Omame & Festus Abiodun Oguntolu

To cite this article: A. El-Mesady, Olumuyiwa James Peter, Andrew Omame & Festus Abiodun Oguntolu (10 Jul 2024): Mathematical analysis of a novel fractional order vaccination model for Tuberculosis incorporating susceptible class with underlying ailment, International Journal of Modelling and Simulation, DOI: 10.1080/02286203.2024.2371684

To link to this article: https://doi.org/10.1080/02286203.2024.2371684

INTERNATIONAL JOURNAL OF MODELLING AND SIMULATION
https://doi.org/10.1080/02286203.2024.2371684

Taylor & Francis
Taylor & Francis Group

Mathematical analysis of a novel fractional order vaccination model for Tuberculosis incorporating susceptible class with underlying ailment

A. El-Mesady[a], Olumuyiwa James Peter[b,c], Andrew Omame[d,e] and Festus Abiodun Oguntolu[f]

[a]Department of Physics and Engineering Mathematics, Faculty of Electronic Engineering, Menoufia University, Menouf, Egypt; [b]Department of Mathematical and Computer Sciences, University of Medical Sciences, Ondo City, Nigeria; [c]Department of Epidemiology and Biostatistics, School of Public Health, University of Medical Sciences, Ondo City, Nigeria; [d]Department of Mathematics, Federal University of Technology Owerri, Imo state, Nigeria; [e]Abdus Salam School of Mathematical Sciences, Government College University, Lahore, Pakistan; [f]Department of Mathematics, Federal University of Technology Minna, Minna, Niger

ABSTRACT

Tuberculosis (TB) is a communicable, airborne infection caused by the bacillus Mycobacterium tuberculosis. Pulmonary tuberculosis (PTB) is the most common presentation, although infection can spread anywhere to cause extra-pulmonary tuberculosis (EPTB). In this paper, a novel fractional order mathematical model is designed for the transmission dynamics of tuberculosis. Uninfected vulnerable individuals are categorized into the following: susceptible with underline ailment and susceptible without underline ailment. The research seeks to qualitatively and quantitatively analyze the proposed model and suggests comprehensive intervention measures for the control of tuberculosis among individuals with underline ailment. Some of the major highlights from the numerical investigation points out that TB vaccination is key to reducing the spread of TB among individuals with underline ailment. Furthermore, efforts to step down the spread of TB through awareness campaigns could significantly reduce the burden of the disease among individuals with co-morbidity.

ARTICLE HISTORY
Received 18 November 2023
Accepted 18 June 2024

KEYWORDS
Epidemics; equilibrium points; stability; fractional caputo derivatives; local stability

1. Introduction

Tuberculosis (TB) is a communicable, airborne infection caused by the bacillus Mycobacterium tuberculosis. Pulmonary tuberculosis (PTB) is the most common presentation, although infection can spread anywhere to cause extra-pulmonary tuberculosis (EPTB). TB is both preventable and curable but limited access to diagnostic and treatment options in some regions remains a significant challenge. The spread of drug-resistant TB, meanwhile, is a continuing global public health crisis [1]. A quarter of the world's population is infected with TB [1], affecting all countries and all ages.

Most cases are asymptomatic and noninfectious (latent TB infection (LTBI)), with an average lifetime transformation risk to active disease of around 10%. An estimated 10 million (8.9–11.0 million) people globally became unwell with TB in 2019, including 1.2 million children. One of these, 8.2% were co-infected with HIV,1 and 1.4 million people died, of whom 208,000 were living with HIV.1 TB incidence rates, however, have been falling, with an estimated 2% decrease per year since 2015 [1].

Globally, an estimated 10.0 million people developed TB disease in 2019, and there were an estimated 1.2 million TB deaths among HIV-negative people and an additional 208, 000 deaths among people living with HIV. Adults accounted for 88% and children for 12 of people with TB. The WHO regions of South-East Asia (44%), Africa (25%), and the Western Pacific (18%) had the most people with TB. Eight countries accounted for two-thirds of the global total: India (26%) Indonesia (8.5%), China (8.4%), the Philippines (6.0%), Pakistan (5.7%), Nigeria (4.4%), Bangladesh (3.6%) and South Africa (3.6%). Only 30% of the 3.5 million five-year target for children treated for TB was met [3]. Major advances have been the development of all new oral regimens for MDRTB and new regimens for preventive therapy. In 2020, the COVID-19 pandemic dislodged TB from the top infectious disease cause of mortality globally. Notably, global TB control efforts were not on track even before the advent of the COVID-19 pandemic. Many challenges remain to improve sub-optimal TB treatment and prevention services. Tuberculosis screening and diagnostic test services need to be ramped up. The major drivers of TB remain under-nutrition, poverty, diabetes, tobacco smoking, and household air pollution and these need to be addressed to achieve the

CONTACT Olumuyiwa James Peter peterjames4real@gmail.com Department of Mathematical and Computer Sciences, University of Medical Sciences, Ondo City, Ondo State, Nigeria
Supplemental data for this article can be accessed online at https://doi.org/10.1080/02286203.2024.2371684

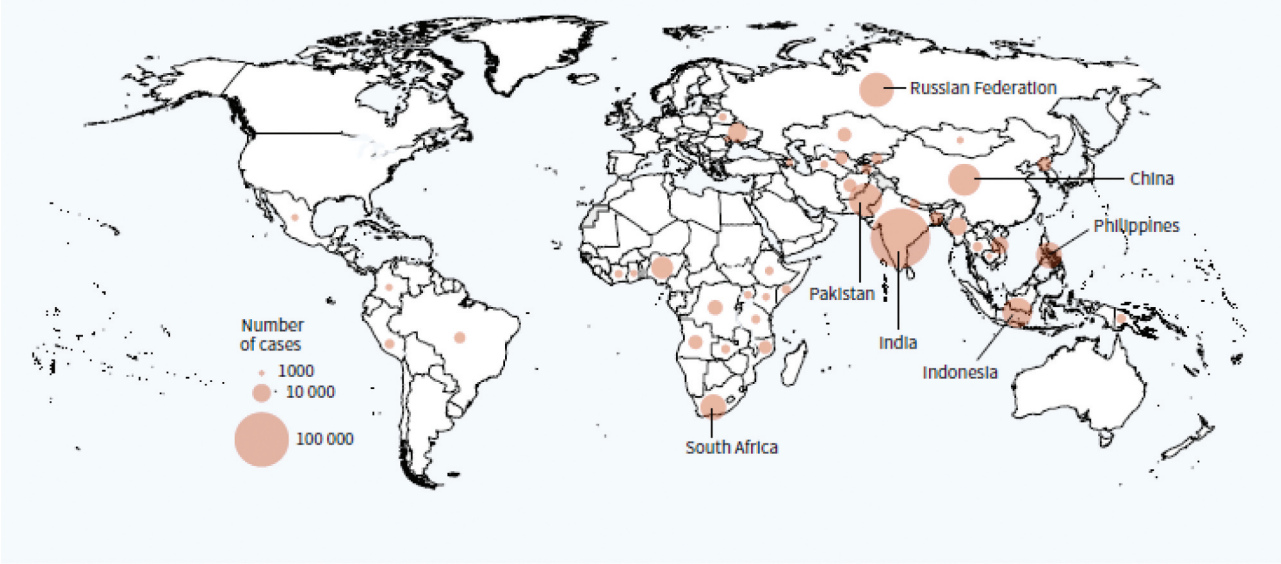

Figure 1. Estimated TB incidence in 2021, for countries with at least 100,000 incident cases:The countries that rank first to eighth in terms of numbers of cases, and that accounted for about two thirds of global cases in 2021, are labelled. Source [2].

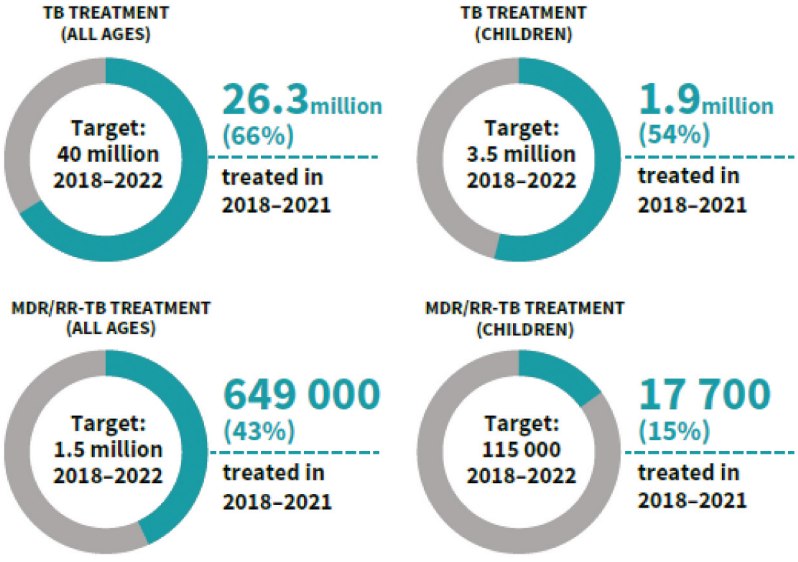

Figure 2. Global progress in the number of people treated for TB between 2018 and 2021, compared with cumulative targets set for 2018–2022 at the UN high-level meeting on TB. Source [2].

WHO 2035 TB care and prevention targets. National programs need to include interventions for post-tuberculosis holistic wellbeing [3]. The estimated TB incidence in 2021, for countries with at least 100,000 incident cases is presented in Figure 1, while the global progress in the number of people treated for TB between 2018 and 2021, compared with cumulative targets set for 2018–2022 at the UN high-level meeting on TB, is depicted by Figure 2.

Mathematical models have become veritable tools for understanding many biological systems such as the dynamics of epidemic diseases. Studies carried out in the past have greatly employed the classical integer order derivatives to gain useful insight into epidemiological models [4–8]. Some of these integer models have been used to understand the dynamics of different diseases, such as tuberculosis [9], COVID-19 [10–12], HIV and syphilis [13], dengue [14], zika [15] and malaria infections [16]. The authors [4] applied an integer model to analyze the triple infection of Zika, dengue and COVID-19. Also, Omame et al. [5] studied the integer model of co-infection involving COVID-19 and dengue. Despite the wide use of integer derivatives to model infectious diseases, they are limited due to the fact that they cannot easily capture

memory effects. Meanwhile, memory effect relates to the fact that the future state of an operator due to the fact that they cannot be on the current state and the past state of a given time-dependent system [17,18]. Hence, a proper understanding of the past dynamics of the disease could facilitate the control of the proliferation of the disease in future [19]. The inclusion of this memory property has motivated research with fractional differential equations [20]. Fractional derivative is at the center stage of epidemiological modeling [21–27].

Motivated by the above research, this paper seeks to investigate a novel fractional-order vaccination model for tuberculosis, categorizing uninfected vulnerable individuals into: susceptibles with underline ailment and susceptibles without underline ailment. The research seeks to qualitatively and quantitatively analyze the novel mathematical model and suggests comprehensive intervention measures for the control of tuberculosis among individuals with underline ailment.

2. Definitions and fundamentals

Definition 2.1 [28]. *For a continuous function* $v:[0,+\infty)\to\mathbb{R}$, *the Riemann–Liouville fractional integral can be defined as*

$$ {}_0^{RL}I_t^{\omega}v(t)=\frac{1}{\Gamma(\omega)}\int_0^t(t-\tau)^{\omega-1}v(\tau)d\tau,\omega\in(0,1),t>0. \tag{2.1}$$

Definition 2.2 [28]. *For a continuous function* $v:[0,+\infty)\to\mathbb{R}$, *the Riemann–Liouville fractional derivative can be defined as*

$$ {}_0^{RL}D_t^{\omega}v(t)=\frac{1}{\Gamma(1-\omega)}\frac{d}{dt}\int_0^t(t-\tau)^{-\omega}v(\tau)d\tau,\omega\in(0,1),t>0. \tag{2.2}$$

Definition 2.3 [28]. *The Caputo fractional derivative for a continuous function* $v:[0,+\infty)\to\mathbb{R}$ *is defined by*

$$ {}_0^{C}D_t^{\omega}v(t)=\frac{1}{\Gamma(1-\omega)}\int_0^t(t-\tau)^{-\omega}\frac{d}{d\tau}v(\tau)d\tau,\omega\in(0,1),t>0. \tag{2.3}$$

Definition 2.4 [28] *Suppose that* $V(s)$ *is the Laplace transform of* $v(t)$. *Then, the Laplace transform of the Caputo fractional derivative is defined as*

$$ \mathcal{L}\left\{{}_O^{C}D_t^{\omega}v(t)\right\}=s^{-\omega}V(s)-\sum_{k=1}^{n-1}s^{\omega-k-1}v^{(k)}(0),\quad (n-1<\omega\le n);n\in N. \tag{2.4}$$

Definition 2.5. *For* $x\in\mathbb{C}$, *the generalized Mittag-Leffler function* $E_{l,m}(x)$ *can be defined by*

$$ E_{l,m}(x)=\sum_{n=0}^{\infty}\frac{x^n}{\Gamma(ln+m)},l>0,m>0, \tag{2.5}$$

and satisfies the following property [28]:

$$ E_{l,m}(x)=xE_{l,l+m}(x)+\frac{1}{\Gamma(m)}. $$

In addition, the Laplace transformation of $t^{m-1}E_{l,m}(\pm\lambda t^l)$ is defined by

$$ L(t^{m-1}E_{l,m}(\pm\lambda t^l))=\frac{s^{l-m}}{s^l\mp\lambda}. \tag{2.6}$$

3. Model formulation

We consider a seven compartmental model in this study based on the epidemiological status of individuals in the population. The population under consideration are $S_1(t)$, this represents susceptible population, $S_2(t)$ represents susceptible individuals to TB with underlying ailment, $V(t)$ represents vaccinated population, $L(t)$ represents Latent population, $I(t)$ represent Active TB population, $T(t)$ represents treated population, and $R(t)$ represents recovered population. Recruitment rate into $S_1(t)$ and $S_2(t)$ are at the rate ϕ_1 and ϕ_2 respectively. We assume that only active TB individuals $I(t)$ can transmit TB infection, thus the force of infection for $S_1(t)$ and $S_2(t)$ are given as $\alpha_1 S_1 I$ and $\alpha_2 S_2 I$. The vaccine wane rate for both $S_1(t)$ and $S_2(t)$ is τ_1 and τ_2 respectively and the rate of vaccination is at a rate ρ. Since the vaccine is not 100% effective, we assume that vaccinated individuals can be infected with TB at a reduced rate $(1-\varepsilon)$ and the force of infection is $(\alpha_1+\alpha_2)\ (1-\varepsilon)VI$. The parameter θ represents the progression rate from latent to active TB class, infected population with TB are treated at a rate γ_1 and γ_2 represent the recovery rate of treated individuals. The term $(1-\omega)\delta_1 T$, where ω represent treatment failure rate, the parameter δ_1 represents the movement rate out of the treated compartment, however, when $\omega=0$, it means the treated individual become latent due to the presence of TB bacteria and the rest of the population become infected due to treatment failure. We assume that, irrespective of individual status, natural death rate can occur at a rate μ and the TB induced death is at rate δ_2 occurs only at the active TB individuals. The above illustration can be represented in a system of nonlinear differential equation in (3.1) in the schematic illustration is presented in Figure 3, while the parameter values and description are given in Table 1.

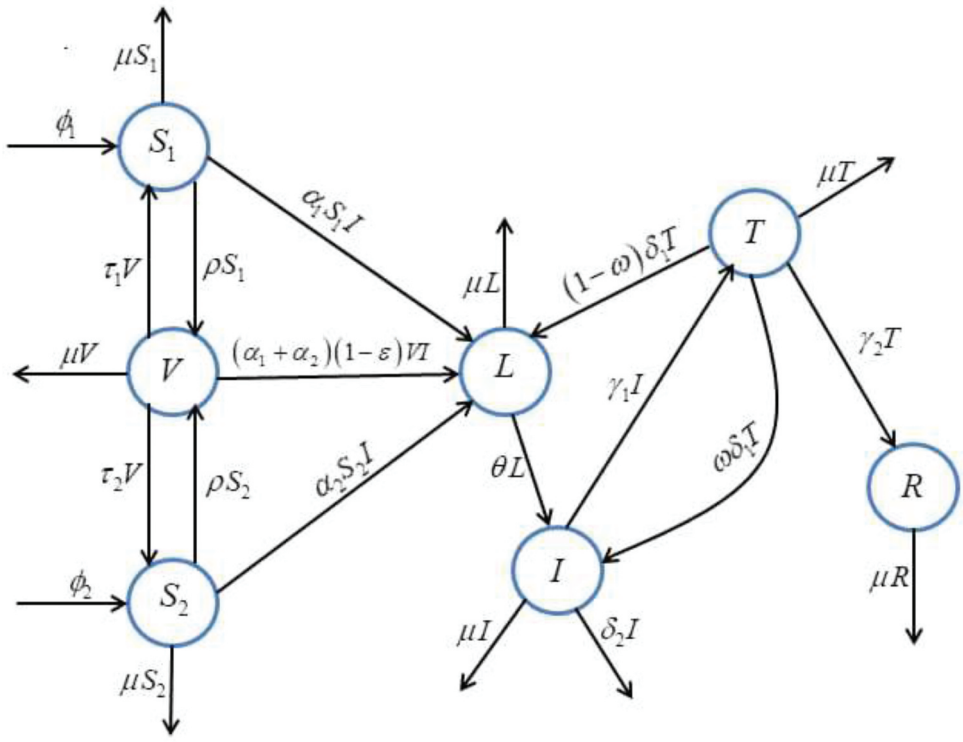

Figure 3. Schematic diagram.

$$\begin{cases} {}_0^C D_t^\alpha S_1(t) = \phi_1 + \tau_1 V - \alpha_1 S_1 I - (\rho+\mu)S_1, \\ {}_0^C D_t^\alpha S_2(t) = \phi_2 + \tau_2 V - \alpha_2 S_2 I - (\rho+\mu)S_2, \\ {}_0^C D_t^\alpha V(t) = \rho(S_1+S_2) - (\alpha_1+\alpha_2)(1-\varepsilon) \\ \qquad VI - (\tau_1+\tau_2+\mu)V, \\ {}_0^C D_t^\alpha L(t) = \alpha_1 S_1 I + \alpha_2 S_2 I + (\alpha_1+\alpha_2)(1-\varepsilon) \\ \qquad VI + (1-\omega)\delta_1 T - (\theta+\mu)L, \\ {}_0^C D_t^\alpha I(t) = \theta L + \omega\delta_1 T - (\mu+\delta_2+\gamma_1)I, \\ {}_0^C D_t^\alpha T(t) = \gamma_1 I - (\delta_1+\mu+\gamma_2)T, \\ {}_0^C D_t^\alpha R(t) = \gamma_2 T - \mu R. \end{cases} \tag{3.1}$$

Table 1. Model parameter values and description.

Parameter	Description	Value	Source
ϕ_1	Recruitment rate into S_1	0.2	Estimated
ϕ_2	Recruitment rate into S_2	0.05	Estimated
α_1	Transmission rate for S_1 and susceptible class	0.6501	[29]
α_2	Transmission rate for S_1 and susceptible class	0.6501	[29]
ρ	Vaccination rate of susceptible class	0.1–0.98	[29]
τ_1	vaccine wane rate for S_1	0.067	[29]
τ_2	vaccine wane rate for S_2	0.0670	[29]
μ	Natural death rate	0.01	[30]
ε	Vaccine efficacy	0–1	[29]
δ_2	TB induced death rate	0.1	[29]
θ	Progression rate from latent to active TB class	0.00375	[29]
γ_1	Treatment rate of infected class	0.1	[31]
γ_2	Recovery rate of treated individuals	0.3968	[31]
ω	Treatment failure rate	0.1500	[31]
δ_1	Movement rate out of treated class	1.1996	[31]

4. Model analysis

4.1. Existence, uniqueness, positivity, and boundedness for solutions

Lemma 4.1 [32]. *Consider the system*

$$ {}_{t_0}^C D_t^\alpha x(t) = g(t, x(t)), t > t_0 \tag{4.1}$$

with initial condition x_{t_0}, *where* $\alpha \in (0,1], g : [t_0, \infty) \times \mho \to \mathbb{R}^n, \mho \in \mathbb{R}^n$, *if* $g(t, x(t))$ *satisfies the locally Lipschitz condition with respect to x, then there exists a unique solution of (4.2) on* $[t_0, \infty) \times \mho \to \mathbb{R}^n$.

Now, we study the existence and uniqueness for the solution of system (4.1) in the region $[t_0, T] \times \mho$, where

$$= \{(S_1, S_2, V, L, I, T, R) \in {}^7 : \max\{|S_1|, |S_2|, |V|, |L|, |I|, |T|, |R|\}\eta\}$$

and $T < +\infty$. We denote $X = (S_1, S_2, V, L, I, T, R)$ and $\bar{X} = (\bar{S}_1, \bar{S}_2, \bar{V}, \bar{L}, \bar{I}, \bar{T}, \bar{R})$. Consider a mapping defined in the following form:

$$G(X) = (G_1(X), G_2(X), G_3(X), G_4(X), G_5(X), G_6(X), G_7(X)), \tag{4.2}$$

where the elements on the right-hand side are defined as

$$\begin{cases} G_1(X) = \phi_1 + \tau_1 V - \alpha_1 S_1 I - (\rho+\mu)S_1, \\ G_2(X) = \phi_2 + \tau_2 V - \alpha_2 S_2 I - (\rho+\mu)S_2, \\ G_3(X) = \rho(S_1+S_2) - (\alpha_1+\alpha_2)(1-\varepsilon) \\ \qquad VI - (\tau_1+\tau_2+\mu)V, \\ G_4(X) = \alpha_1 S_1 I + \alpha_2 S_2 I + (\alpha_1+\alpha_2)(1-\varepsilon) \\ \qquad VI + (1-\omega)\delta_1 T - (\theta+\mu)L, \\ G_5(X) = \theta L + \omega\delta_1 T - (\mu+\delta_2+\gamma_1)I, \\ G_6(X) = \gamma_1 I - (\delta_1+\mu+\gamma_2)T, \\ G_7(X) = \gamma_2 T - \mu R. \end{cases} \tag{4.3}$$

For any , it follows from (4.2) and (4.7) that

$$\begin{aligned} ||G(X) - G(\bar{X})|| = \\ |G_1(X) - G_1(\bar{X})| + |G_2(X) - G_2(\bar{X})| + \\ |G_3(X) - G_3(\bar{X})| + |G_4(X) - G_4(\bar{X})| + \\ |G_5(X) - G_5(\bar{X})| + |G_6(X) - G_6(\bar{X})| + \\ |G_7(X) - G_7(\bar{X})| \le H||X - \bar{X}||, \end{aligned} \tag{4.4}$$

where
$H = \max\{2\alpha_1\eta + 2\rho + \mu, 2\alpha_2\eta + 2\rho + \mu, 2\tau_1 + 2\tau_2 + 2(\alpha_1+\alpha_2)(1-\varepsilon)\eta + \mu, 2\theta + \mu, 2\alpha_1\eta + 2\alpha_2\eta + 2(\alpha_1+\alpha_2)(1-\varepsilon)\eta + 2\gamma_1 + \mu + \delta_2, 2\delta_1 + 2\omega\delta_1 + \mu + 2\gamma_2, \mu\}$. Thus, $G(X)$ satisfies the Lipschitz condition. It follows from Lemma (4.1) that there exists a unique solution $X(t)$ of system (3.1) with initial condition

$$X_{t_0} = (S_1(0), S_2(0), V(0), L(0), I(0), T(0), R(0)) \tag{4.5}$$

Consequently, we have the following theorem:

Theorem 4.2. *For each initial condition $X_{t_0} \in \mho$, there exists a unique solution $X(t) \in \mho$, to the fractional order system (3.1), which is defined for all $t \ge t_0$.*

In order to demonstrate the boundedness and nonnegativity of the solution for the model (3.1) for all time $t \ge t_0$, provided that the initial conditions and all other parameters are taken to be positive, we introduce the generalized mean values theorem [33] in this section. To do this, we must start with the subsequent lemma.

Lemma 4.3. *Let $g(t)$ and ${}^{C}_{t_0}D^{\alpha}_t g(t)$ belong to $C[t_0, t_f]$. Then, we get*

$$g(t) = g(t_0) + \frac{1}{\Gamma(\alpha)_{t_0}} {}^{C}D^{\alpha}_{\xi} g(\xi).(t-t_0)^{\alpha}, t_0 \le \xi \le t, \forall t \in (t_0, t_f]. \tag{4.6}$$

Corollary 4.4. *Let $g(t)$ and ${}^{C}_{t_0}D^{\alpha}_t g(t)$ belong to $C[t_0, t_f]$, and $\alpha \in (0,1]$. From Lemma (4.1) if*

(i) ${}^{C}_{t_0}D^{\alpha}_t g(t) 0, \quad t \in (t_0, t_f]$, then $g(t)$ is non-decreasing $t \in (t_0, t_f]$.
(ii) ${}^{C}_{t_0}D^{\alpha}_t g(t) 0, \quad t \in (t_0, t_f]$, then $g(t)$ is non-increasing $t \in (t_0, t_f]$.

Theorem 4.5. *For the model (3.1), the region $\Omega_+ = \{(S_1, S_2, V, L, I, T, R), S_1 > 0, S_2 > 0, V \ge 0, L \ge 0, I \ge 0, T \ge 0, R \ge 0\}$ is a positive invariant.*

Proof: From the model (3.1), we have

$$\begin{cases} {}^{C}_{0}D^{\alpha}_t S_1(t)|_{S_1=0} = \phi_1 + \tau_1 > V, \\ {}^{C}_{0}D^{\alpha}_t S_2(t)|_{S_2=0} = \phi_2 + \tau_2 > V, \\ {}^{C}_{0}D^{\alpha}_t V(t)|_{V=0} = \rho(S_1+S_2) \ge 0, \\ {}^{C}_{0}D^{\alpha}_t L(t)|_{L=0} = \alpha_1 S_1 I + \alpha_2 S_2 I + (\alpha_1+\alpha_2)(1-\varepsilon) \\ \qquad VI + (1-\omega)\delta_1 T \ge 0, \\ {}^{C}_{0}D^{\alpha}_t I(t)|_{I=0} = \theta L + \omega\delta_1 T \ge 0, \\ {}^{C}_{0}D^{\alpha}_t T(t)|_{T=0} = \gamma_1 I \ge 0, \\ {}^{C}_{0}D^{\alpha}_t R(t)|_{R=0} = \gamma_2 T \ge 0. \end{cases} \tag{4.7}$$

The region Ω_+ is a positive invariant, according to Corollary 4.4 and model (3.1). The solution will therefore remain inside Ω_+.

To demonstrate the solution's boundedness, the following theorem is presented.

Theorem 4.6. *The region $\Omega = \{(S_1, S_2, V, L, I, T, R), 0 < N \le \frac{\phi_1+\phi_2}{\mu}$ is a positive invariant set for the model (3.1).*

Proof: Adding the equations of the model (3.1) gives

$${}^{C}_{0}D^{\alpha}_t N(t) = \phi_1 + \phi_2 - \mu N(t) - \delta_2 I(t), \tag{4.8}$$

that can be rewritten as follows

$${}^{C}_{0}D^{\alpha}_t N(t) \le \phi_1 + \phi_2 - \mu N(t), \tag{4.9}$$

The Laplace transform is then applied to equation (4.9), which results in

$$s^{\alpha}\bar{N}(s) - s^{\alpha-1}N(0) \le \frac{\phi_1+\phi_2}{s} - \mu\bar{N}(s) \tag{4.10}$$

The preceding equation can be expressed as follows:

$$\bar{N}(s) \le \frac{s^{-1}}{s^{\alpha}+\mu}(\phi_1+\phi_2) + \frac{s^{\alpha-1}}{s^{\alpha}+\mu}N(0). \tag{4.11}$$

If $(S_1(0), S_2(0), V(0), L(0), I(0), T(0), R(0)) \in \Omega$, then we arrive at the following by using equations (2.5) and (2.6),

$$N(t) \le (\phi_1+\phi_2)t^{\alpha}E_{\alpha,\alpha+1}(-\mu t^{\alpha}) + E_{\alpha,1}(-\mu t^{\alpha})N(0), \tag{4.12}$$

$$N(t) \leq (\phi_1 + \phi_2)t^{\alpha}E_{\alpha,\alpha+1}(-\mu t^{\alpha}) + E_{\alpha,1}(-\mu t^{\alpha})\frac{(\phi_1 + \phi_2)}{\mu}, \tag{4.13}$$

$$N(t) \leq (\phi_1 + \phi_2)\mu(\mu t^{\alpha}E_{\alpha,\alpha+1}(-\mu t^{\alpha}) + E_{\alpha,1}(-\mu t^{\alpha})), \tag{4.14}$$

$$N(t) \leq \frac{(\phi_1 + \phi_2)}{\mu}\left(-\left(E_{\alpha,\alpha+1}(-\mu t^{\alpha}) - \frac{1}{\Gamma(1)}\right) + E_{\alpha,1}(-\mu t^{\alpha})\right), \tag{4.15}$$

$$N(t) \leq \frac{\phi_1 + \phi_2}{\mu}. \tag{4.16}$$

Hence, based on Theorem 4.5 and relation (4.16), we get $0 < N(t)\phi_1 + \phi_2\mu$. The region Ω is hence positively invariant. Consequently, the proposed model's solution is bounded, and has mathematical and epidemiological importance.

4.2. The model and its equilibria and stability

The description of how the equilibrium points of the discussed model (3.1) was derived is provided below. The equilibrium points are first determined, after which the model's stability is examined. The solution to the following equations determine the equilibria of the discussed model (3.1):

$$\begin{cases} \phi_1 + \tau_1 V - \alpha_1 S_1 I - (\rho + \mu)S_1 = 0, \\ \phi_2 + \tau_2 V - \alpha_2 S_2 I - (\rho + \mu)S_2 = 0, \\ \rho(S_1 + S_2) - (\alpha_1 + \alpha_2)(1 - \varepsilon) \\ \qquad VI - (\tau_1 + \tau_2 + \mu)V = 0, \\ \alpha_1 S_1 I + \alpha_2 S_2 I + (\alpha_1 + \alpha_2)(1 - \varepsilon) \\ \quad VI + (1 - \omega)\delta_1 T - (\theta + \mu)L = 0, \\ \theta L + \omega\delta_1 T - (\mu + \delta_2 + \gamma_1)I = 0, \\ \gamma_1 I - (\delta_1 + \mu + \gamma_2)T = 0, \\ \gamma_2 T - \mu R = 0. \end{cases} \tag{4.17}$$

Hence, we obtain the disease-free equilibrium point which is

$$\begin{cases} S_1^* = \frac{\phi_1(\tau_1(\mu+\rho)+\mu(\mu+\rho+\tau_2))+\rho\tau_1\phi_2}{\mu(\mu+\rho)(\mu+\rho+\tau_1+\tau_2)}, \\ S_2^* = \frac{\mu\phi_2(\mu+\rho+\tau_1)+\tau_2(\phi_2(\mu+\rho)+\rho\phi_1)}{\mu(\mu+\rho)(\mu+\rho+\tau_1+\tau_2)}, \\ V^* = \frac{\rho(\phi_1+\phi_2)}{\mu(\mu+\rho+\tau_1+\tau_2)}, \\ L^* = 0, \\ I^* = 0, \\ T^* = 0, \\ R^* = 0, \end{cases} \tag{4.18}$$

and endemic equilibrium point which is

$$\begin{cases} S_1^{**} = \frac{\gamma_1\gamma_2(-\tau_1 V^{**} - \phi_1)}{-\gamma_1\gamma_2\mu - \gamma_1\gamma_2\rho - \alpha_1\gamma_2\mu R^{**} - \alpha_1\delta_1\mu R^{**} - \alpha_1\mu^2 R^{**}}, \\ S_2^{**} = \frac{\gamma_1\gamma_2(-\tau_2 V^{**} - \phi_2)}{-\gamma_1\gamma_2\mu - \gamma_1\gamma_2\rho - \alpha_2\gamma_2\mu R^{**} - \alpha_2\delta_1\mu R^{**} - \alpha_2\mu^2 R^{**}}, \\ V^{**} = \frac{\frac{\gamma_1\gamma_2\rho\phi_1}{-\gamma_1\gamma_2\mu - \gamma_1\gamma_2\rho - \alpha_1\gamma_2\mu R^{**} - \alpha_1\delta_1\mu R^{**} - \alpha_1\mu^2 R^{**}} + \frac{\gamma_1\gamma_2\rho\phi_2}{-\gamma_1\gamma_2\mu - \gamma_1\gamma_2\rho - \alpha_2\gamma_2\mu R^{**} - \alpha_2\delta_1\mu R^{**} - \alpha_2\mu^2 R^{**}}}{-\mu - \frac{\gamma_1\gamma_2\rho\tau_1}{-\gamma_1\gamma_2\mu - \gamma_1\gamma_2\rho - \alpha_1\gamma_2\mu R^{**} - \alpha_1\delta_1\mu R^{**} - \alpha_1\mu^2 R^{**}} - \frac{\gamma_1\gamma_2\rho\tau_2}{-\gamma_1\gamma_2\mu - \gamma_1\gamma_2\rho - \alpha_2\gamma_2\mu R^{**} - \alpha_2\delta_1\mu R^{**} - \alpha_2\mu^2 R^{**}} - \frac{(\alpha_1+\alpha_2)\mu R^{**}(1-\varepsilon)(\gamma_2+\delta_1+\mu)}{\gamma_1\gamma_2} - \tau_1 - \tau_2}, \\ L^{**} = \frac{\mu R^{**}(-\gamma_1\delta_1\omega + \gamma_1\delta_1 + \gamma_2\delta_2 + \gamma_1\mu + \gamma_2\mu + \gamma_1\gamma_2 + \delta_1\mu + \delta_2\mu + \delta_1\delta_2 + \mu^2)}{\gamma_1\gamma_2\theta}, \\ I^{**} = \frac{\mu R^{**}(\gamma_2+\delta_1+\mu)}{\gamma_1\gamma_2}, \\ T^{**} = \frac{\mu R^{**}}{\gamma_2}, \\ R^{**} \end{cases} \tag{4.19}$$

where R^{**} can be found by solving the complicated algebraic equation in Appendix A.

The Jacobian $\mathfrak{J}$ of equation (3.1) can be represented by the following matrix.

$$\mathfrak{J} = \begin{pmatrix} -\mu-\rho-\alpha_1 I & 0 & \tau_1 & 0 & -\alpha_1 S_1 & 0 & 0 \\ 0 & -\mu-\rho-\alpha_2 I & \tau_2 & 0 & -\alpha_2 S_2 & 0 & 0 \\ \rho & \rho & A & 0 & C & 0 & 0 \\ \alpha_1 I & \alpha_2 I & B & -\theta-\mu & D & -\delta_1(\omega-1) & 0 \\ 0 & 0 & 0 & \theta & -\gamma_1-\delta_2-\mu & \delta_1\omega & 0 \\ 0 & 0 & 0 & 0 & \gamma_1 & -\gamma_2-\delta_1-\mu & 0 \\ 0 & 0 & 0 & 0 & 0 & \gamma_2 & -\mu \end{pmatrix}, \tag{4.20}$$

$$\begin{cases} A = -\mu - \tau_1 - \tau_2 + (\alpha_1 + \alpha_2)(\varepsilon - 1)I, \\ B = (\alpha_1 + \alpha_2)(1 - \varepsilon)I, \\ C = (\alpha_1 + \alpha_2)(\varepsilon - 1)V, \\ D = \alpha_1 S_1 + \alpha_2 S_2 - (\alpha_1 + \alpha_2)(\varepsilon - 1)V. \end{cases} \tag{4.21}$$

4.3. The equilibrium points' stability

The following system

$$\begin{cases} {}_0^c D_t^{\alpha} S_1(t) = \phi_1 + \tau_1 V - \alpha_1 S_1 I - (\rho + \mu)S_1, \\ {}_0^c D_t^{\alpha} S_2(t) = \phi_2 + \tau_2 V - \alpha_2 S_2 I - (\rho + \mu)S_2, \\ {}_0^c D_t^{\alpha} V(t) = \rho(S_1 + S_2) - (\alpha_1 + \alpha_2)(1 - \varepsilon) \\ \qquad VI - (\tau_1 + \tau_2 + \mu)V, \\ {}_0^c D_t^{\alpha} L(t) = \alpha_1 S_1 I + \alpha_2 S_2 I + (\alpha_1 + \alpha_2)(1 - \varepsilon) \\ \qquad VI + (1 - \omega)\delta_1 T - (\theta + \mu)L, \\ {}_0^c D_t^{\alpha} I(t) = \theta L + \omega\delta_1 T - (\mu + \delta_2 + \gamma_1)I, \\ {}_0^c D_t^{\alpha} T(t) = \gamma_1 I - (\delta_1 + \mu + \gamma_2)T, \\ {}_0^c D_t^{\alpha} R(t) = \gamma_2 T - \mu R, \end{cases} \tag{4.22}$$

will be asymptotically stable if all of the resulting Jacobian matrix's eigenvalues fulfil the Matignon requirements

$$|arg(\lambda_i)| > \alpha\pi/2, \tag{4.23}$$

as stated in reference [34]. We will now go over the local stability of each equilibrium point in turn [35]. The Jacobian matrix at the equilibrium with no disease is represented by

$$\Im_1 = \begin{pmatrix} -\mu-\rho & 0 & \tau_1 & 0 & E & 0 & 0 \\ 0 & -\mu-\rho & \tau_2 & 0 & F & 0 & 0 \\ \rho & \rho & -\mu-\tau_1-\tau_2 & 0 & G & 0 & 0 \\ 0 & 0 & 0 & -\theta-\mu & H & -\delta_1(\omega-1) & 0 \\ 0 & 0 & 0 & \theta & -\gamma_1-\delta_2-\mu & \delta_1\omega & 0 \\ 0 & 0 & 0 & 0 & \gamma_1 & -\gamma_2-\delta_1-\mu & 0 \\ 0 & 0 & 0 & 0 & 0 & \gamma_2 & -\mu \end{pmatrix}, \tag{4.24}$$

$$\begin{cases} E = -\frac{\alpha_1(\phi_1(\tau_1(\mu+\rho)+\mu(\mu+\rho+\tau_2))+\rho\tau_1\phi_2)}{\mu(\mu+\rho)(\mu+\rho+\tau_1+\tau_2)}, \\ F = -\frac{\alpha_2(\mu\phi_2(\mu+\rho+\tau_1)+\tau_2(\phi_2(\mu+\rho)+\rho\phi_1))}{\mu(\mu+\rho)(\mu+\rho+\tau_1+\tau_2)}, \\ G = \frac{(\alpha_1+\alpha_2)\rho(\varepsilon-1)(\phi_1+\phi_2)}{\mu(\mu+\rho+\tau_1+\tau_2)}, \\ \quad \alpha_1(\phi_1(\tau_1(\mu+\rho)+\mu(\mu+\rho+\tau_2))+\rho\tau_1\phi_2)+ \\ \quad \alpha_2(\mu\phi_2(\mu+\rho+\tau_1)+\tau_2(\phi_2(\mu+\rho)+\rho\phi_1))+ \\ H = \frac{(\alpha_1+\alpha_2)\rho((1-\varepsilon))(\phi_1+\phi_2)(\mu+\rho)}{\mu(\mu+\rho)(\mu+\rho+\tau_1+\tau_2)} \end{cases} \tag{4.25}$$

The eigenvalues of the Jacobian matrix $\Im_1$ are very complicated. Hence, we use numerical solutions for showing the stability regions of the parameters for the disease-free equilibrium point. Some stability regions of parameters for the disease-free equilibrium point is shown in Figure 4. Similary, the stability regions of parameters for the endemic equilibrium point can be discovered if the complicated equation in Appendix A is solved.

To better understand the spread of disease in the population, we frequently use the concept of the basic reproduction number R_0. The next-generation matrix method is used to find R_0. Hence, R_0 can be given by

$$R_0 = \rho(AB^{-1}) \tag{4.26}$$

where ρ is the spectral radius of the matrix AB^{-1} and A, B^{-1} are as follows:

$$A = \begin{pmatrix} 0 & \alpha_1 S_1 + \alpha_2 S_2 + (\alpha_1+\alpha_2)V(1-\varepsilon) \\ 0 & 0 \end{pmatrix}, \tag{4.27}$$

$$B^{-1} = \begin{pmatrix} \frac{1}{\theta+\mu} & 0 \\ \frac{\theta}{(\theta+\mu)(\gamma_1+\delta_2+\mu)} & \frac{1}{\gamma_1+\delta_2+\mu} \end{pmatrix}, \tag{4.28}$$

the matrix AB^{-1} will have the following form

$$AB^{-1} = \begin{pmatrix} \frac{\theta(\alpha_1 S_1+\alpha_2 S_2+(\alpha_1+\alpha_2)V(1-\varepsilon))}{(\theta+\mu)(\gamma_1+\delta_2+\mu)} & \frac{\alpha_1 S_1+\alpha_2 S_2+(\alpha_1+\alpha_2)V(1-\varepsilon)}{\gamma_1+\delta_2+\mu} \\ 0 & 0 \end{pmatrix}. \tag{4.29}$$

Thus, we have R_0 as

$$R_0 = \frac{\theta\left(\begin{array}{l} \frac{\alpha_1(\phi_1(\tau_1(\mu+\rho)+\mu(\mu+\rho+\tau_2))+\rho\tau_1\phi_2)}{\mu(\mu+\rho)(\mu+\rho+\tau_1+\tau_2)} + \\ \frac{\alpha_2(\mu\phi_2(\mu+\rho+\tau_1)+\tau_2(\phi_2(\mu+\rho)+\rho\phi_1))}{\mu(\mu+\rho)(\mu+\rho+\tau_1+\tau_2)} + \\ \frac{\alpha_1\rho(1-\varepsilon)(\phi_1+\phi_2)}{\mu(\mu+\rho+\tau_1+\tau_2)} + \frac{\alpha_2\rho(1-\varepsilon)(\phi_1+\phi_2)}{\mu(\mu+\rho+\tau_1+\tau_2)} \end{array}\right)}{(\theta+\mu)(\gamma_1+\delta_2+\mu)} \tag{4.30}$$

4.4. Sensitivity index

In this section, the effects induced on the basic reproduction number due to changes in the key model parameters are investigated. This can assist in determining which model parameters have the most effects on R_0 and how changes in those parameters affect the spread of the disease. For a given parameter p, define the sensitivity index $S_p^{R_0}$ of R_0 to p as follows

$$S_p^{R_0} = \frac{\partial R_0}{\partial p} \times \frac{p}{R_0} \tag{4.31}$$

By taking $\alpha = 1$, we get the results shown in Appendix B.

In Figure 5, the sensitivity index of R_0 is calculated for different parameters in the model (3.1). It is depicted that the some parameters have a positive sensitivity index, which indicates that increasing (decreasing) the values of these parameters will result in increasing (decreasing) the value of R_0. Some other parameters have negative sensitivity index which means that increasing (decreasing) the values of these parameters will result in decreasing (increasing) the value of R_0. The remaining parameters have zero sensitivity index which shows that these parameters have no effect on R_0.

5. Numerical simulations

In this section, we demonstrate a numerical solution for the proposed fractional order model. To obtain the numerical solution, we utilize the generalized Adams-Bashforth-Moulton method. This method involves employing a predictor-corrector scheme to compute numerical solutions for nonlinear fractional differential equations (FDEs). We estimate the solution using this method by considering the following subsequent nonlinear FDE:

$${}_0D_t^{\alpha}\psi(t) = g(t, \psi(t)), 0 \le t \le T \tag{5.1}$$

with the given initial conditions as follows:

$$\psi^{(i)}(0) = \psi_0^i, i = 0, 1, 2, \ldots, [\alpha] - 1. \tag{5.2}$$

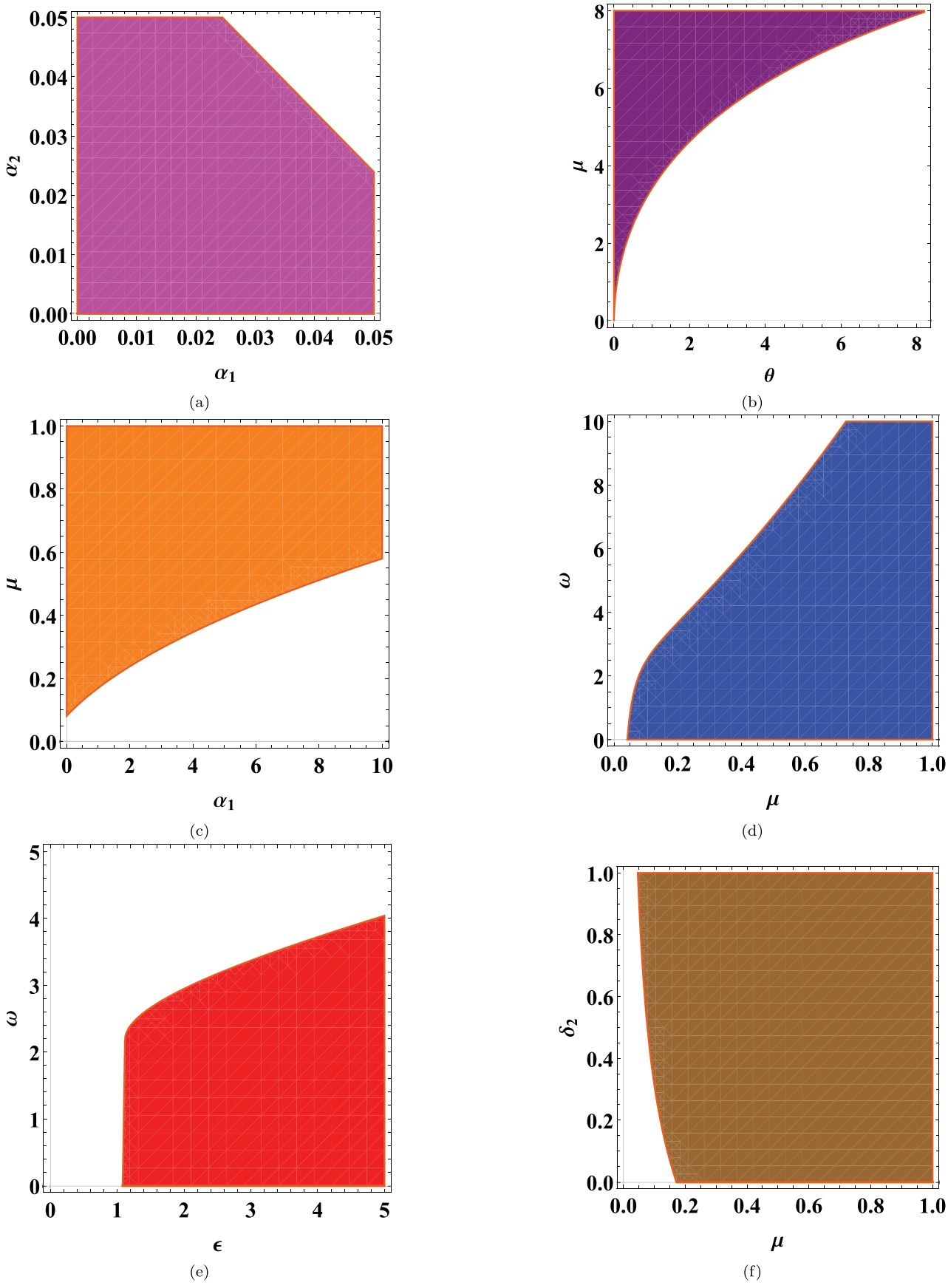

Figure 4. Stability regions of parameters for the disease-free equilibrium point.

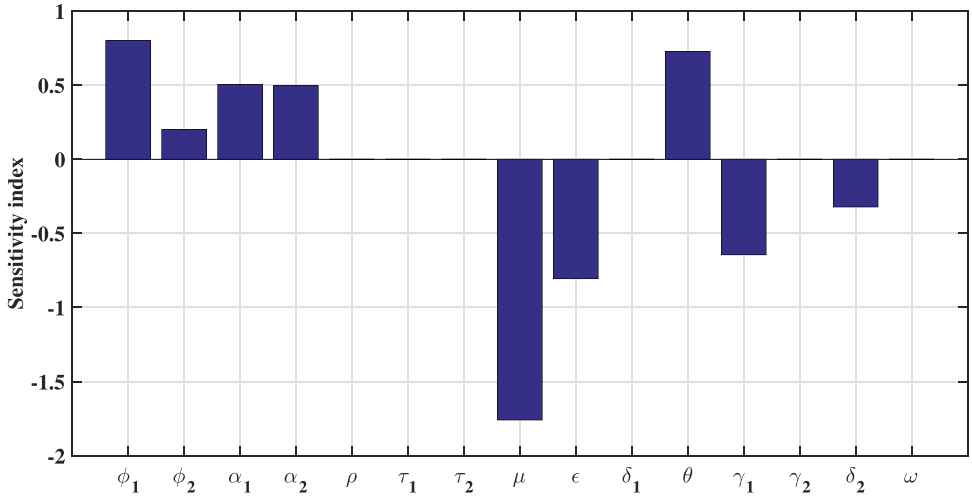

Figure 5. Sensitivity index of R_0 to different parameters in model (3.1).

By solving the following equation and applying the fractional integral operator to Eq. (5.1), we can obtain the solution $\psi(t)$;

$$\psi(t) = \sum_{i=0}^{[\alpha]-1} \frac{\psi_0^i}{i!} t^i + \frac{1}{\Gamma(\alpha)} \int_0^t (t-\xi)^{\alpha-1} g(\xi, \psi(\xi)) d\xi, \tag{5.3}$$

The Volterra integral equation and this equation, Eq. (5.3), are equivalent. Equation (5.3) can be integrated using the predictor-corrector method based on the Adams-Bashforth-Moulton algorithm. Putting $h = TN, t_n = nh$ and $n = 0, 1, 2, \ldots, N \in Z^+$. The discretization of equation (5.4) is as follows:

$$\begin{aligned}\psi_h(t_{n+1}) = &\sum_{i=0}^{[\alpha]-1} \frac{\psi_0^i}{i!} t_{n+1}^i + \frac{h^\alpha}{\Gamma(\alpha+2)} g\left(t_{n+1}, \psi_h^p(t_{n+1})\right) \\ &+ \frac{h^\alpha}{\Gamma(\alpha+2)} \sum_{k=0}^{n} a_{k,n+1}\, g\left(t_k, \psi_h(t_k)\right),\end{aligned} \tag{5.4}$$

where

$$a_{k,n+1} = \begin{cases} n^{\alpha+1} - (n-\alpha)(n+1)^\alpha, \text{if } k = 0, \\ (n-k+2)^{\alpha+1} + (n-k)^{\alpha+1} \\ \quad -2(n-k+1)^{\alpha+1}, \text{if } 0 < k \le n, \\ 1, \text{if } k = n+1 \end{cases} \tag{5.5}$$

where the predicted value $\psi_h^p(t_{n+1})$ is established by

$$\psi_h^p(t_{n+1}) = \sum_{i=0}^{[\alpha]-1} \frac{\psi_0^i}{i!} t_{n+1}^i + \frac{1}{\Gamma(\alpha)} \sum_{k=0}^{n} b_{k,n+1}\, g\left(t_k, \psi_h(t_k)\right), \tag{5.6}$$

with

$$b_{k,n+1} = \frac{h^\alpha}{\alpha}\left((n+1-k)^\alpha - (n-k)^\alpha\right). \tag{5.7}$$

The estimated error is

$$\max_{k=0,1,2,\ldots,m} |\psi(t_k) - \psi_h(t_k)| = O(h^r), \tag{5.8}$$

where $r = \min(2, 1+\alpha)$.

5.1. Disease-free point

The time-series profiles of the different epidemiological compartments at disease-free steady state are presented in Figure 6. It is observed from these experiments, that the solution trajectories tend or converge toward the TB-free steady state. The influence of variation in the order of the fractional derivative is also observed in various epidemiological states. Specifically, it can be observed that increasing the order of the derivative caused corresponding increase in the susceptible (with or without underline ailment) and vaccinated compartments. However, increasing the order of the derivative caused a decline in the infected and recovered populations. In Figures 7 and 8, contour plots of the various compartments as functions of the fractional derivative and time are presented. The figures highlight the impact of memory on the epidemiological classes over time. It is also observed that over time, as the order of the derivative is increased, the susceptible and vaccinated populations increase while the infected and recovered populations decrease over time. The trajectories, irrespective of the order of the derivative, all converge to the TB-free equilibrium. $\phi_1 = 0.2, \phi_2 = 0.05, \alpha_1 = 0.03, \alpha_2 = 0.04, \rho = 0.6,$ $\tau_1 = 0.067, \tau_2 = 0.0670, \mu = 0.01, \varepsilon = 0.5, \delta_2 = 0.1,$ $\theta = 0.00375, \gamma_1 = 0.2, \gamma_2 = 0.3968, \omega = 0.1500,$

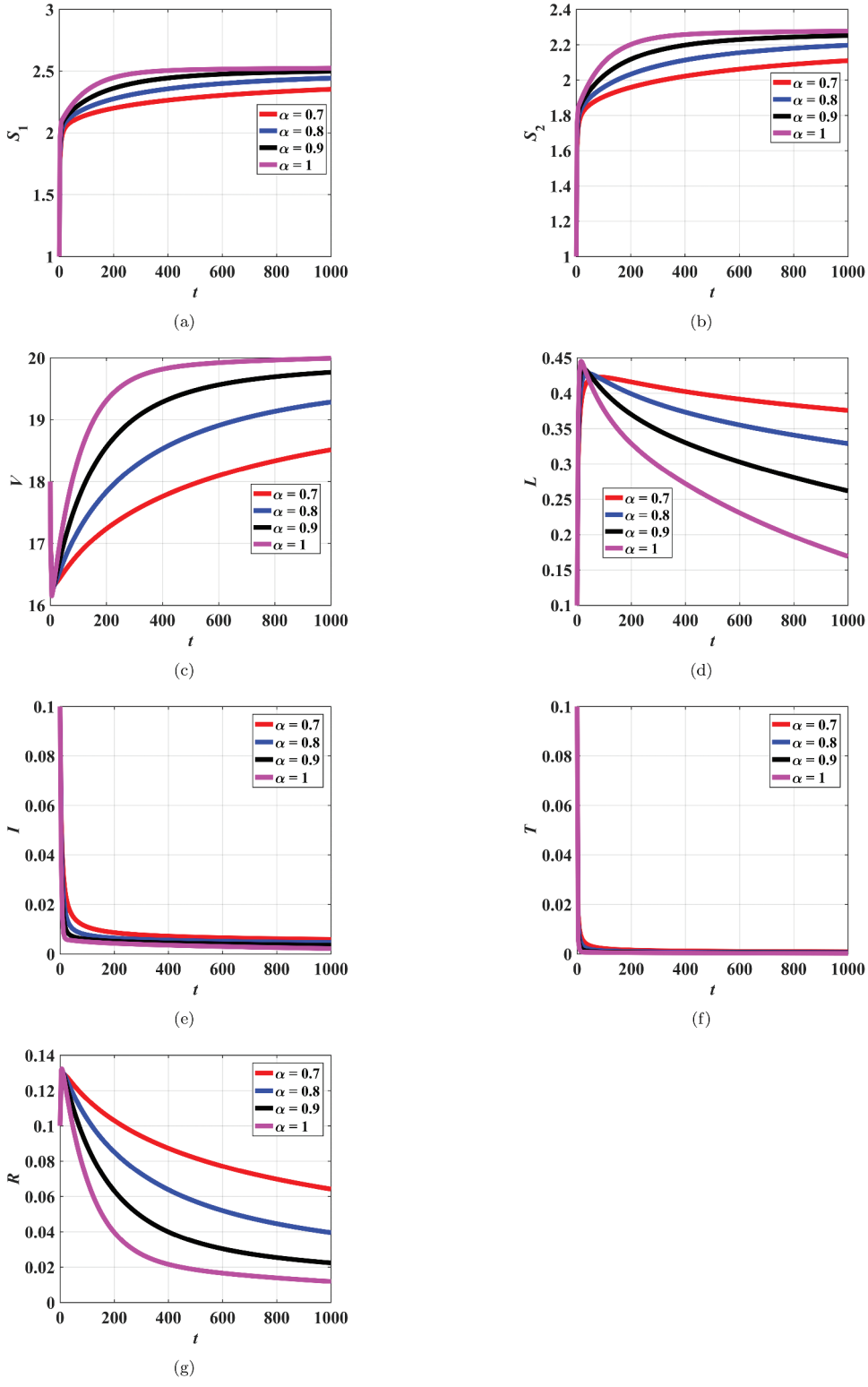

Figure 6. Dynamical behavior of state variables for disease-free case.

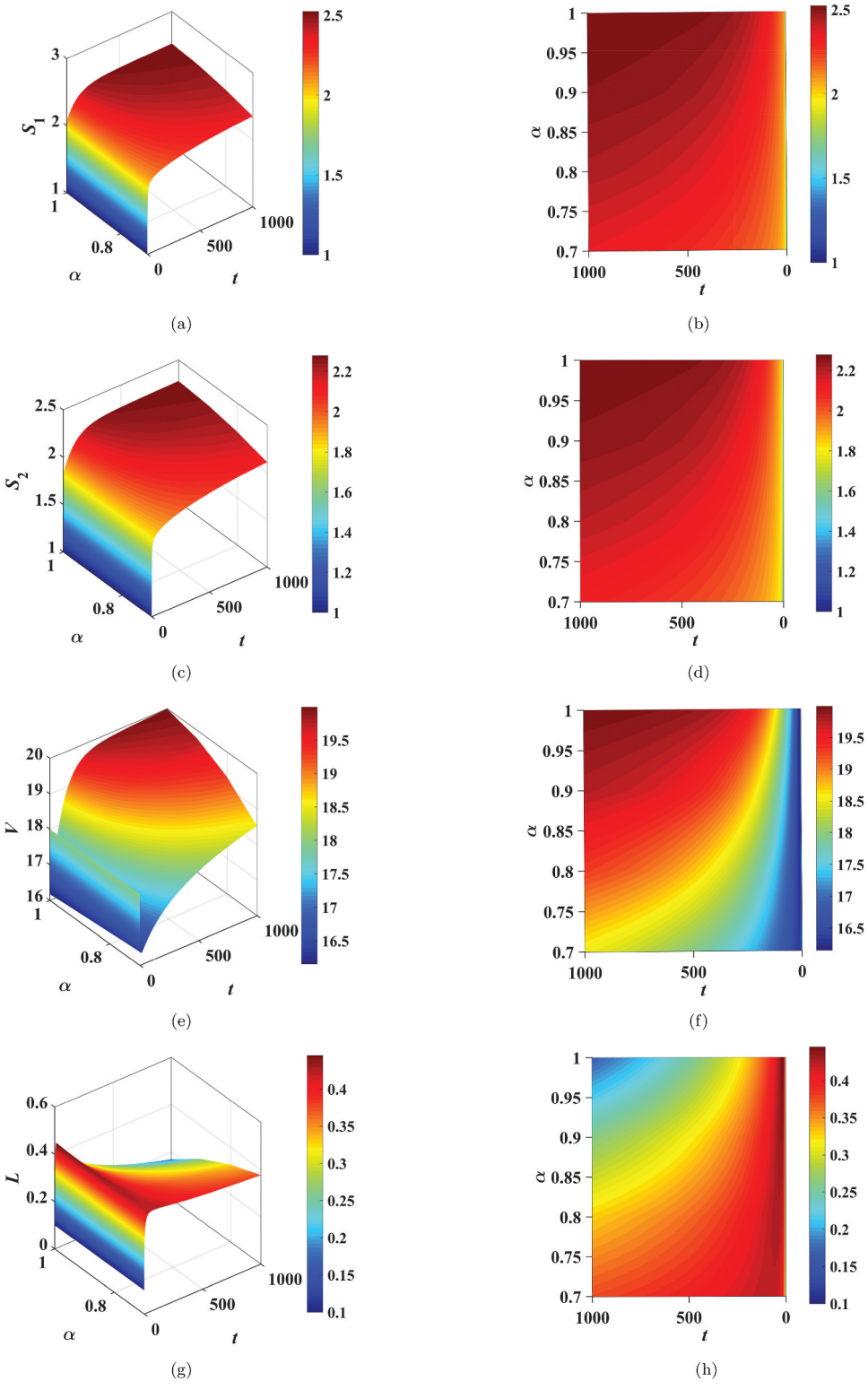

Figure 7. 3D plots of S_1, S_2, V, L populations versus time and fractional order a with the corresponding contour plots for disease-free case.

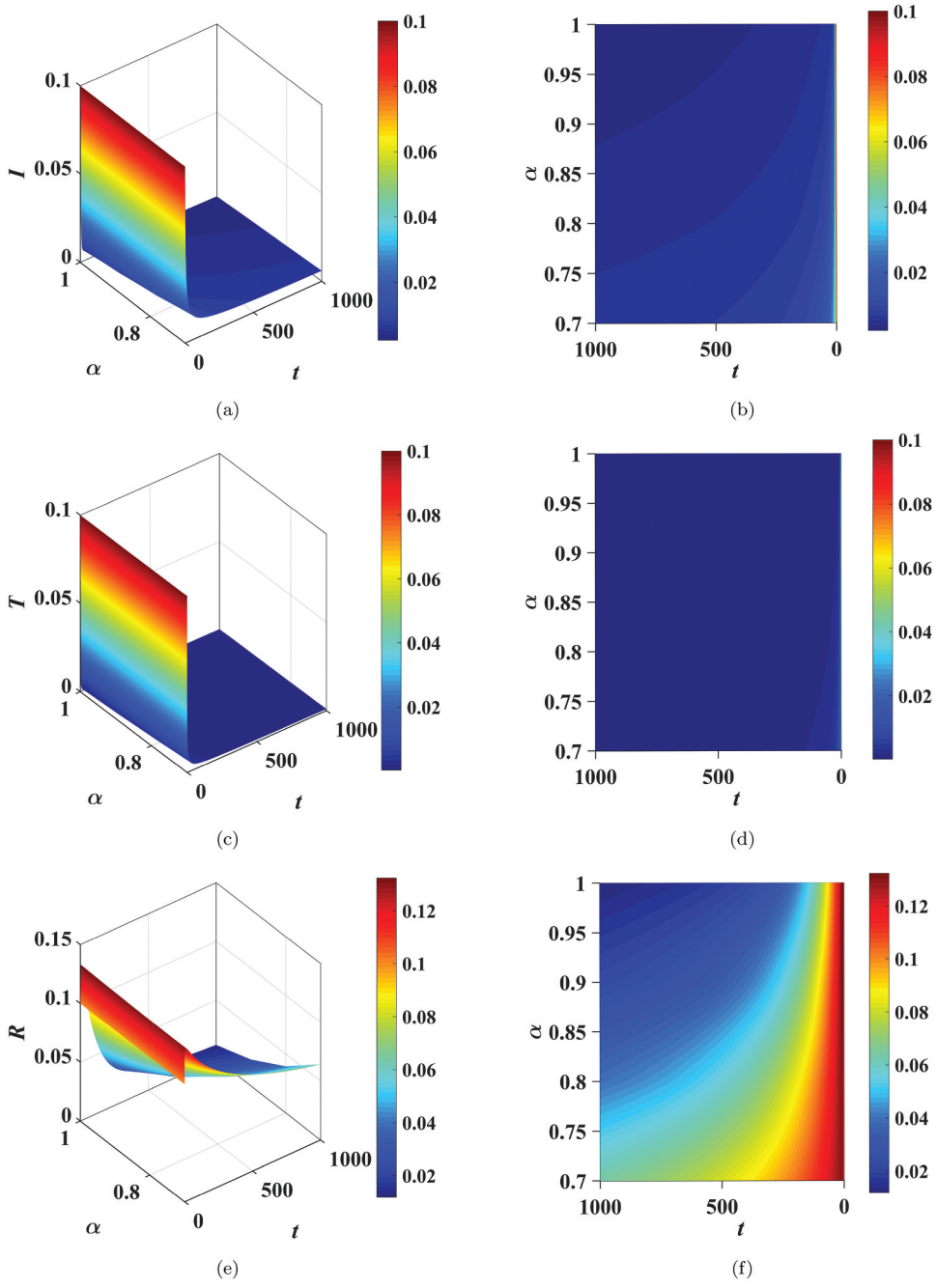

Figure 8. 3D plots of I, T, R populations versus time and fractional order α with the corresponding contour plots for disease-free case.

$\delta_1 = 1.1996, \text{and} S_1(0) = 1, S_2(0) = 1, V(0) = 18,$
$L(0) = 0.1, I(0) = 0.1, T(0) = 0.1, R(0) = 0.1.$

5.2. Endemic point

The time-series profiles of the different epidemiological compartments at TB-endemic steady state are presented in Figure 9. It is observed from these numerical experiments, that the solution trajectories tend towards the TB-endemic steady state. The influence of variation in the order of fractional derivative is also observed in the various epidemiological states. Specifically, it can be observed that increasing the order of the derivative caused corresponding variations in the susceptible (with or without underline ailment) and vaccinated compartments. More-so, increasing the order of the derivative equally caused variations in the infected and recovered populations. In Figures 10 and 11, contour plots of the various compartments as functions of the fractional derivative and time are presented. The figures highlight the impact of memory on the epidemiological classes

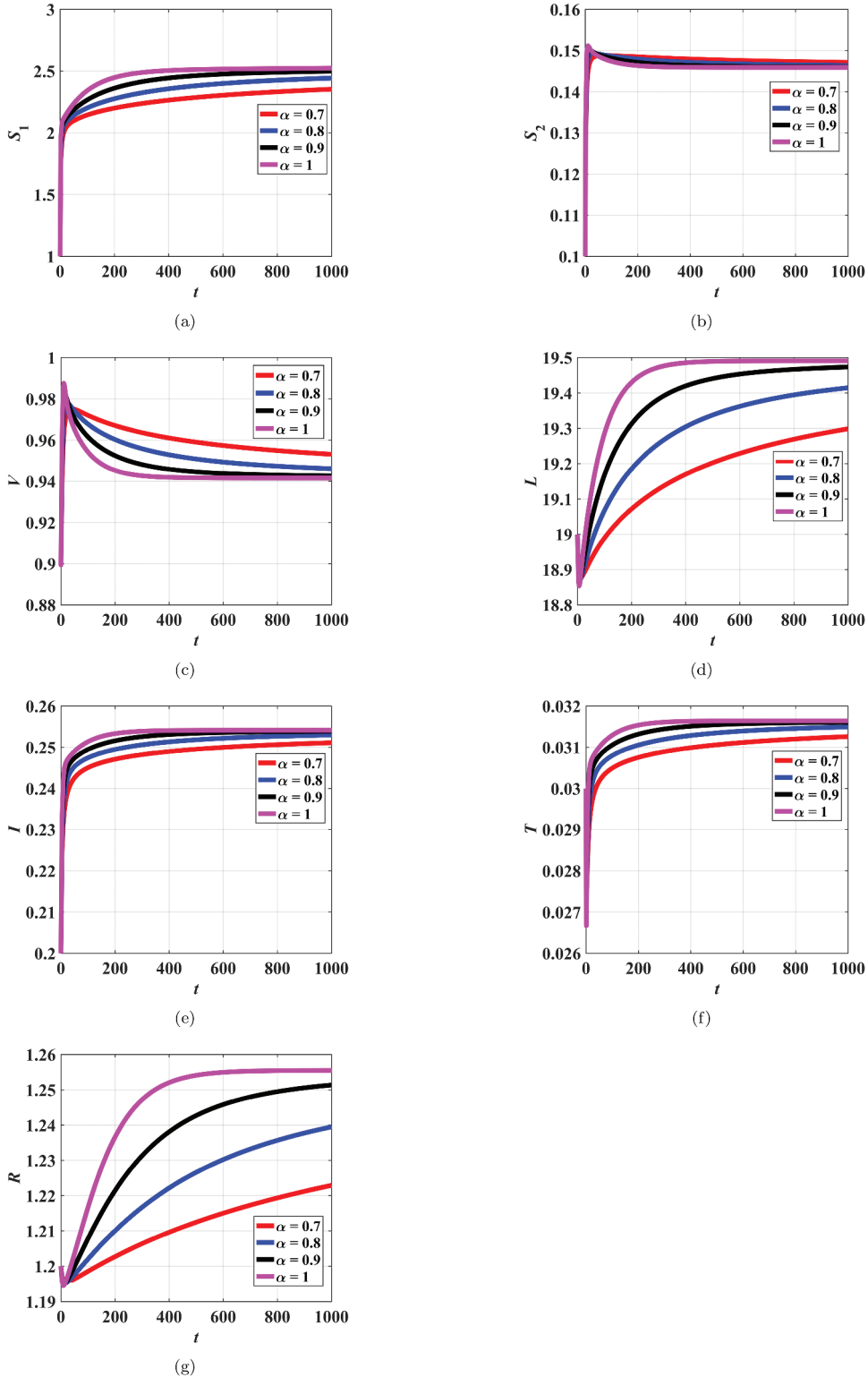

Figure 9. Dynamical behavior of state variables for endemic case.

over time. It is also observed that, the memory effect greatly influenced the population dynamics of the susceptible and vaccinated individuals. Also, the population profiles of infected and recovered individuals are greatly influenced by the memory effect. In addition, the trajectories, irrespective of the order of the fractional derivative, converge to the TB-endemic equilibrium. It is worthy of note to state that, these observations can only be observed in a fractional-order model. The impact of memory on the

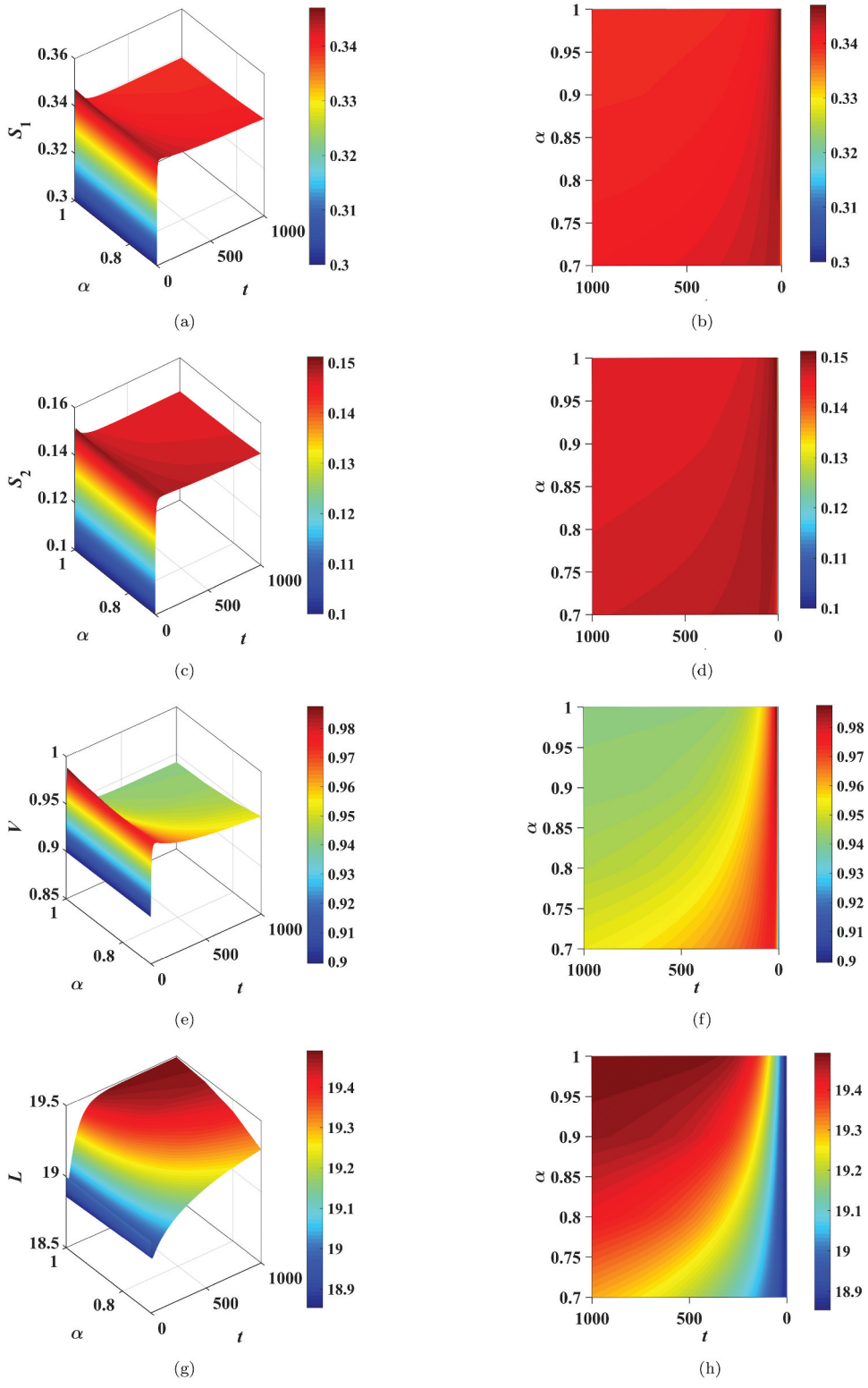

Figure 10. 3D plots of S_1, S_2, V, L populations versus time and fractional order α with the corresponding contour plots for endemic case.

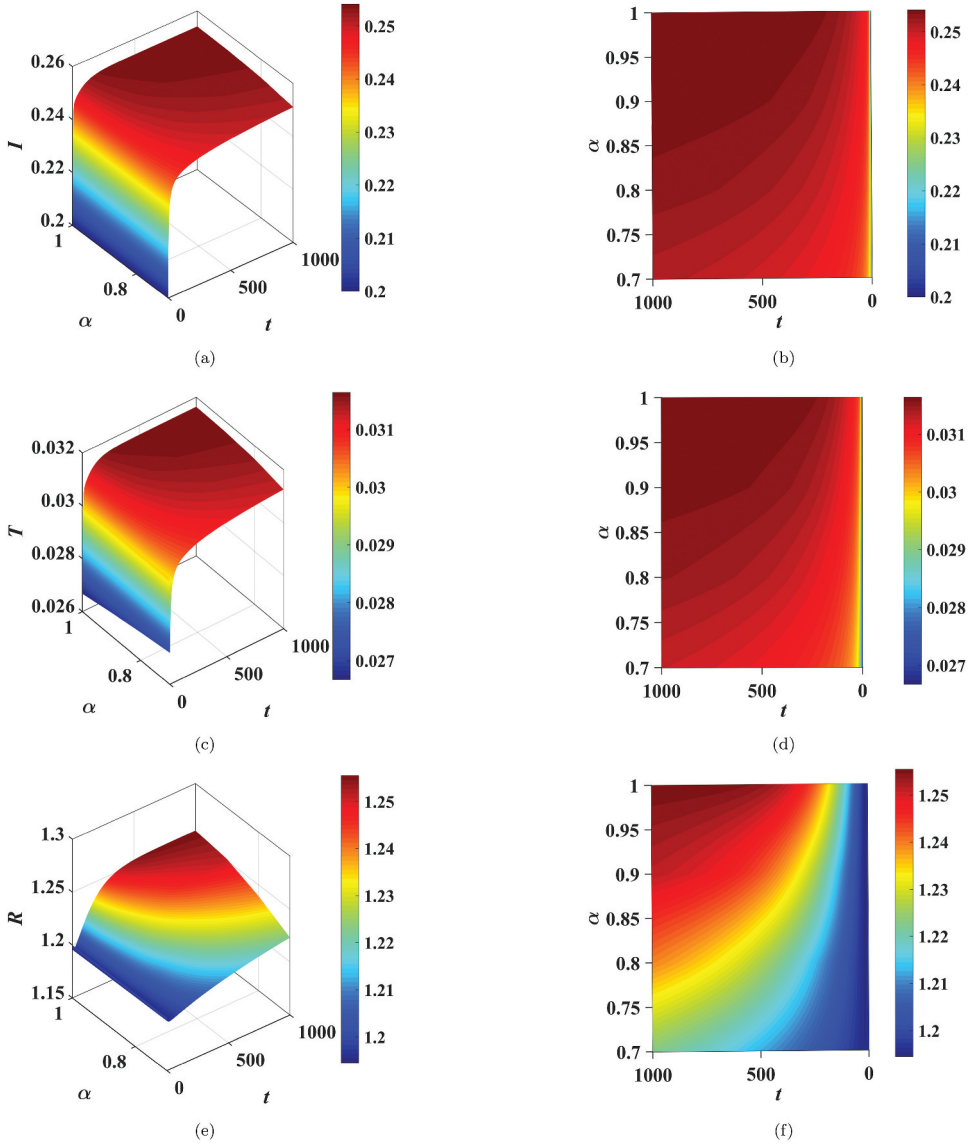

Figure 11. 3D plots of I, T, R populations versus time and fractional order a with the corresponding contour plots for endemic case.

population dynamics of the various epidemiological classes cannot be explained by an integer-order model, as it lacks the memory effect which is only inherent in the definition of a fractional-derivative.

It is also important to state that, the Caputo fractional operator endowed with a singular kernel offers advantages in modeling disease transmissions by providing a more flexible framework that captures memory effects, non-local behavior, and complex dynamics. Memory effects imply that the history of the system is captured. In TB transmission model, this can be particularly useful for capturing the impact of past infections, immunity, or interventions on the current state of the population. Unlike classical derivatives, fractional derivatives are non-local operators showing that the behavior of the system at a particular point in time depends on its history over a range of time, which could be crucial for modeling the spread of tuberculosis since past interactions can greatly influence future outcomes.

$\phi_1 = 0.2, \phi_2 = 0.05, \alpha_1 = 0.6501, \alpha_2 = 0.6501, \rho = 0.6,$
$\tau_1 = 0.067, \tau_2 = 0.0670, \mu = 0.01, \varepsilon = 0.5, \delta_2 = 0.1,$
$\theta = 0.00375, \gamma_1 = 0.2, \gamma_2 = 0.3968, \omega = 0.1500,$
$\delta_1 = 1.1996,$ and $S_1(0) = 0.3, S_2(0) = 0.1,$
$V(0) = 0.9, L(0) = 19, I(0) = 0.2, T(0) = 0.03,$
$R(0) = 1.2.$

5.3. Effect of vaccination measures

We fix all the parameters of the endemic case except the specified parameters under each figure.

In Figures 12–19, simulations of the various classes of the model are presented to assess the impact of

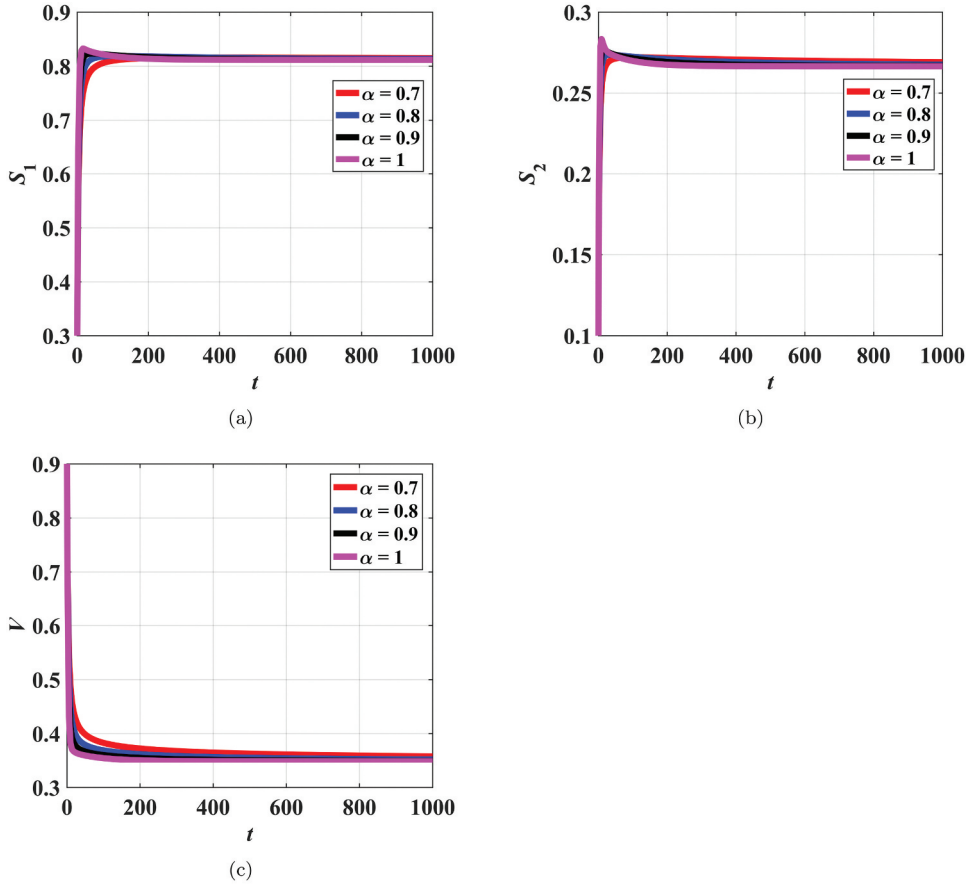

Figure 12. Dynamical behavior of S_1, S_2, V state variables for endemic case when $\rho = 0.1$.

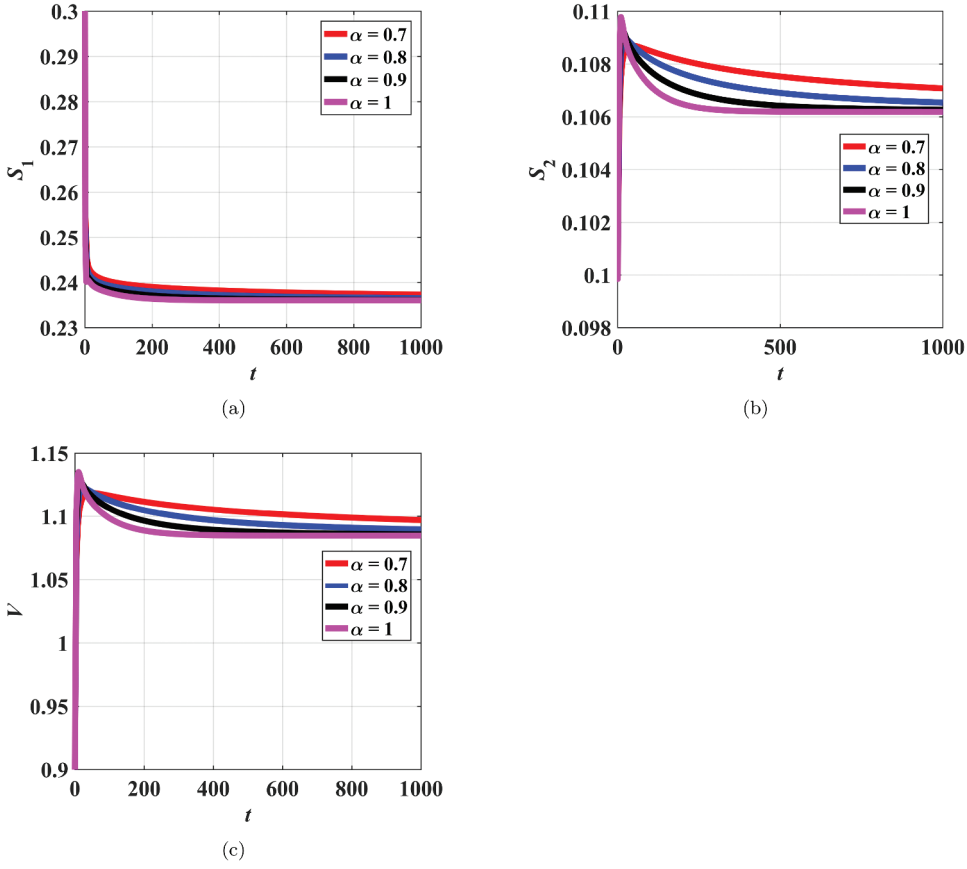

Figure 13. Dynamical behavior of S_1, S_2, V state variables for endemic case when $\rho = 0.98$.

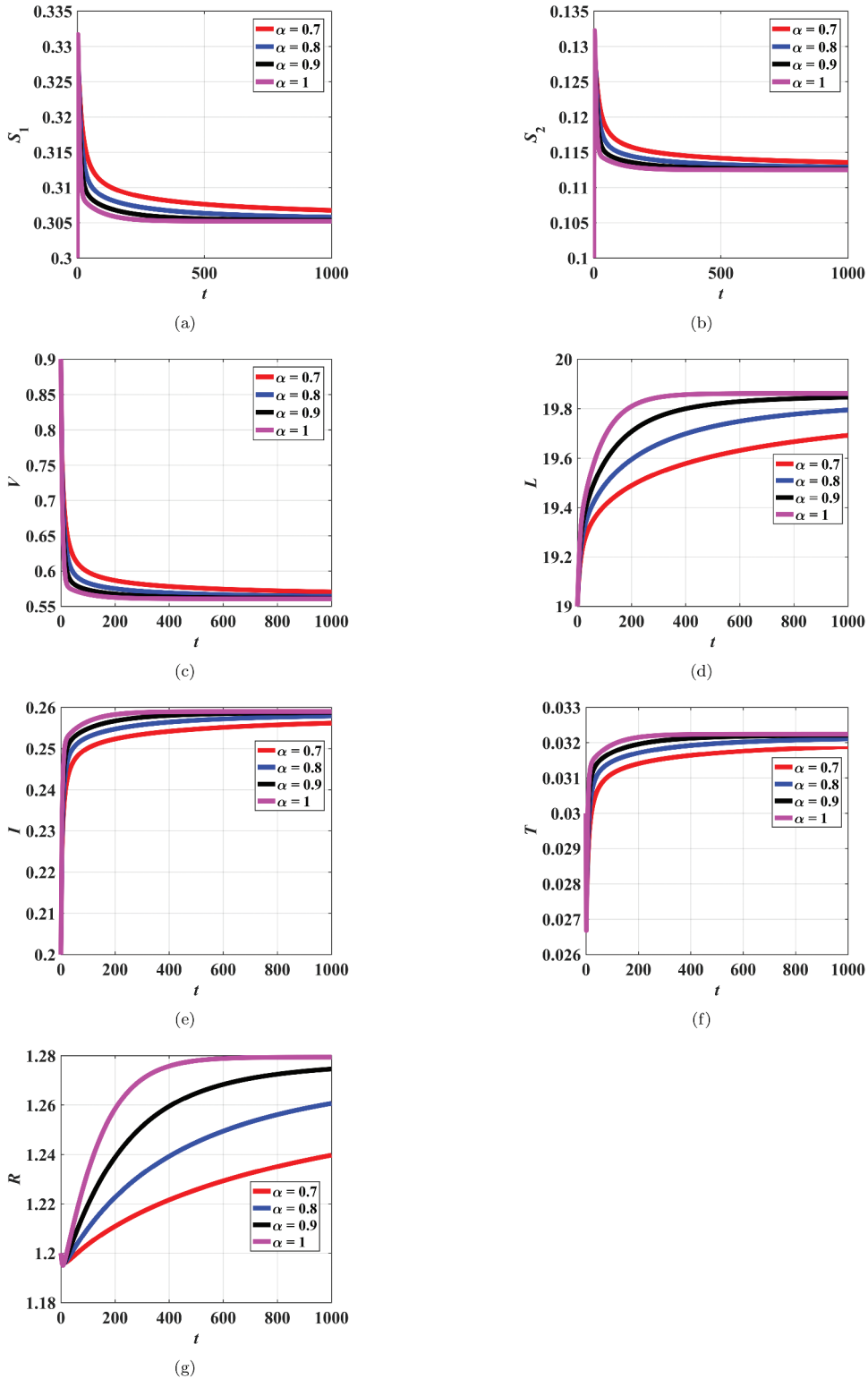

Figure 14. Dynamical behavior of all state variables for endemic case when $\varepsilon = 0.1$.

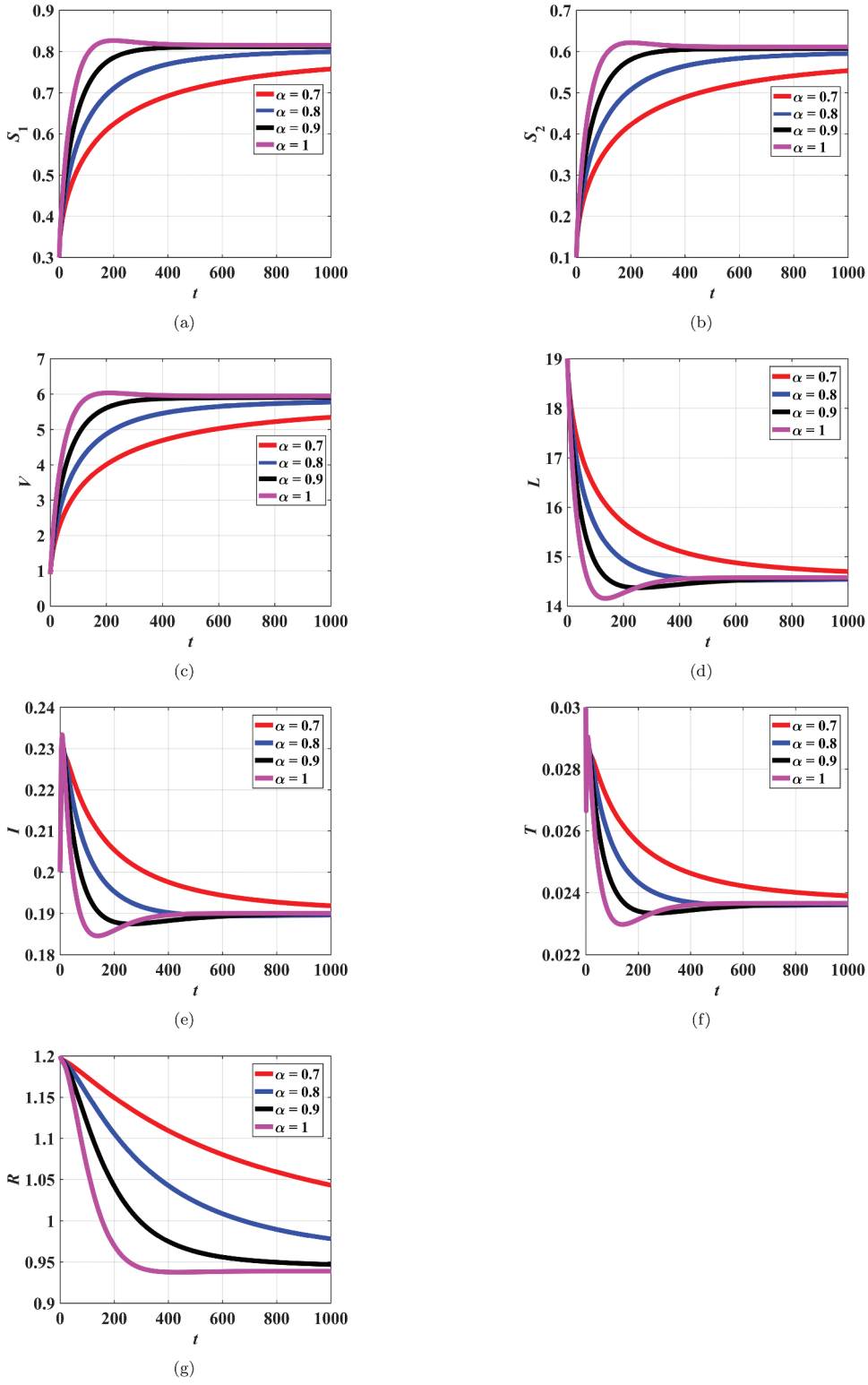

Figure 15. Dynamical behavior of all state variables for endemic case when $\varepsilon = 1$.

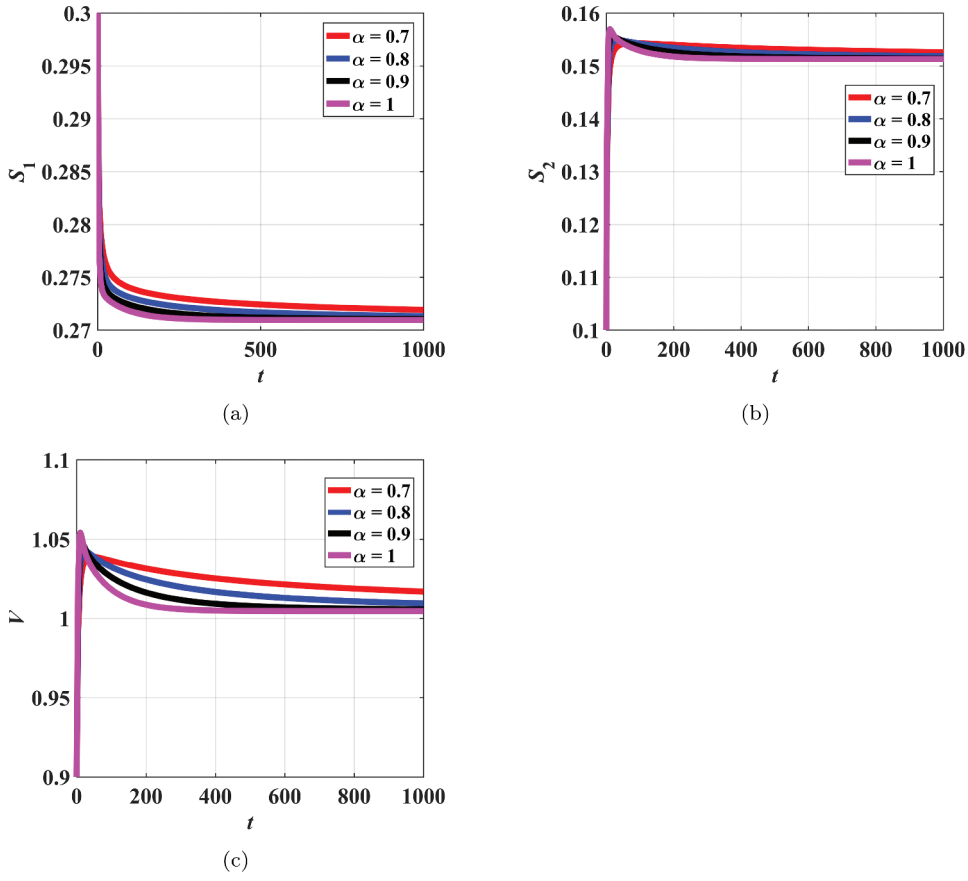

Figure 16. Dynamical behavior of S_1, S_2, V state variables for endemic case when $\tau_1 = 0.01$.

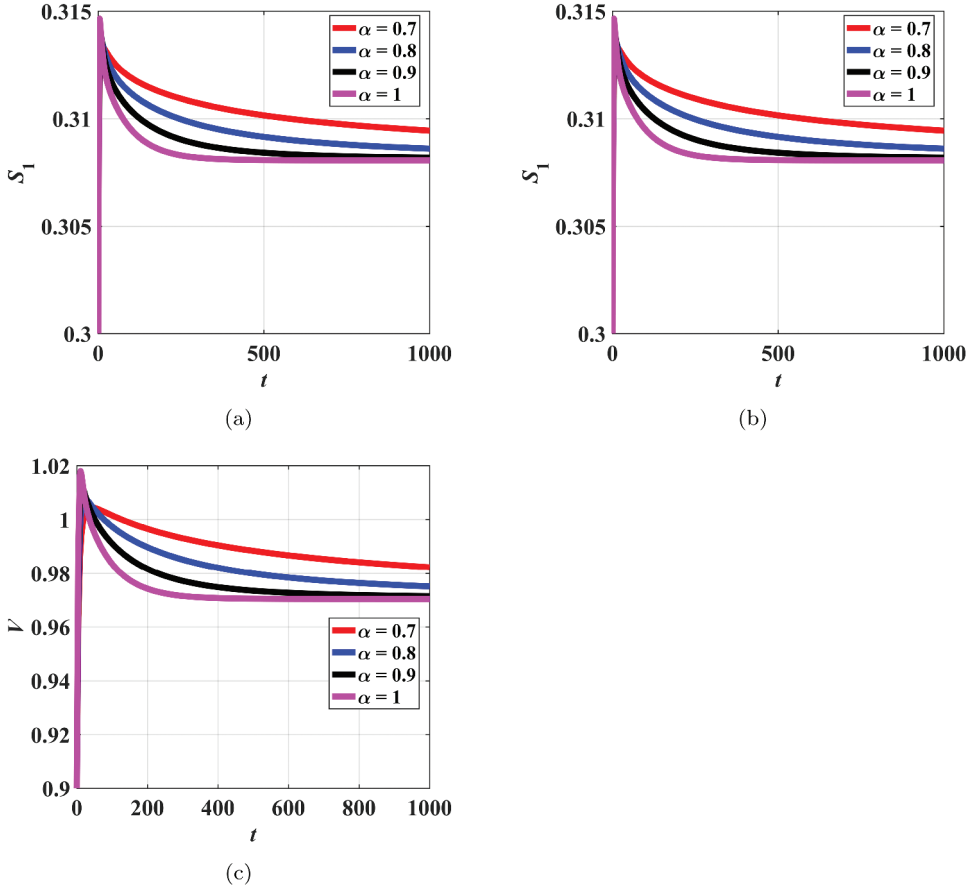

Figure 17. Dynamical behavior of S_1, S_2, V state variables for endemic case when $\tau_1 = 0.04$.

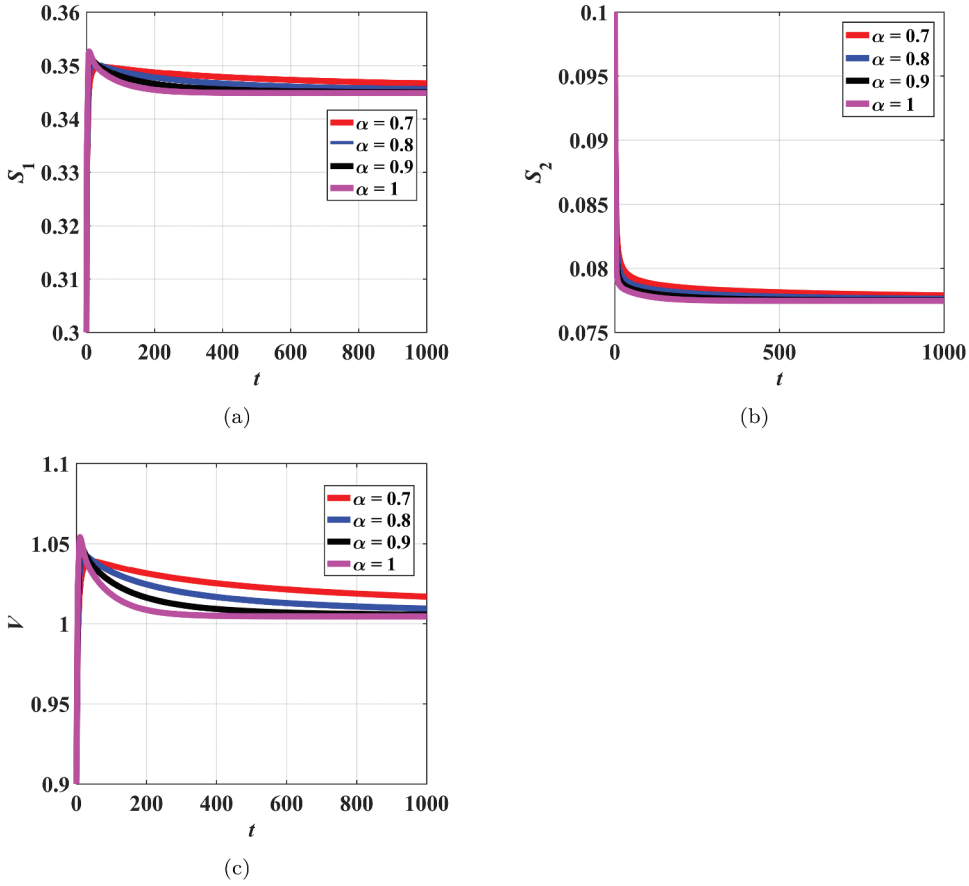

Figure 18. Dynamical behavior of S_1, S_2, V state variables for endemic case when $\tau_2 = 0.01$.

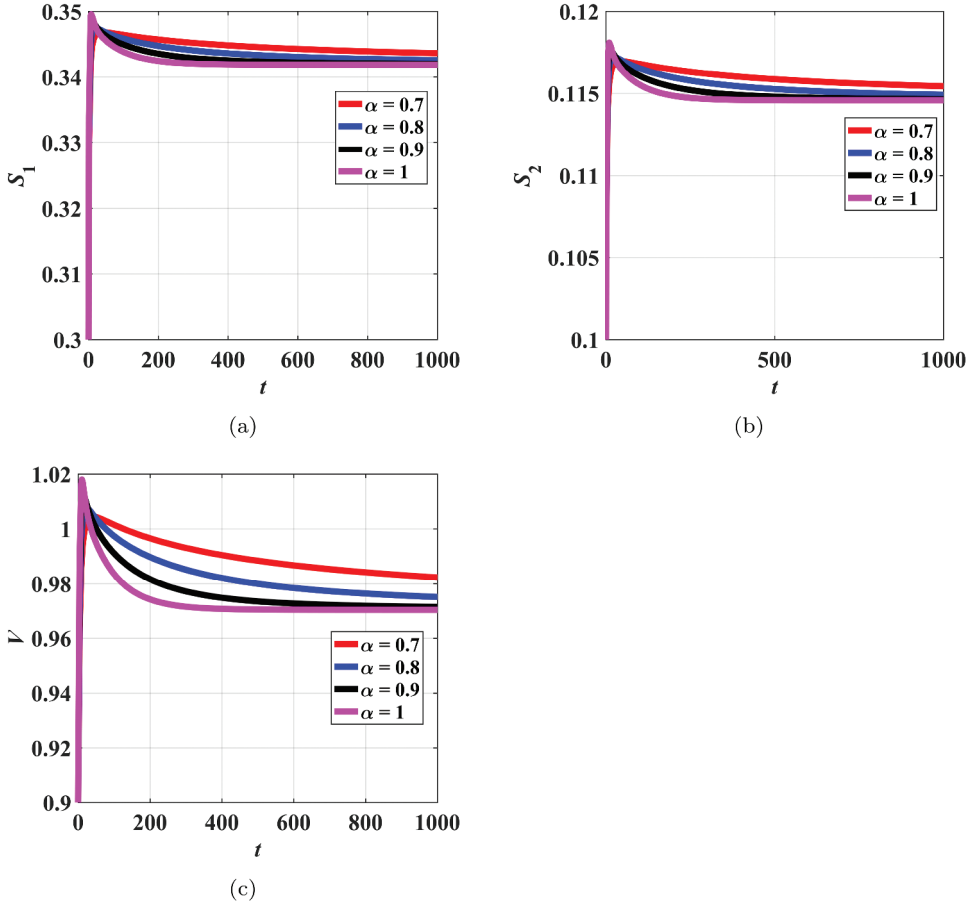

Figure 19. Dynamical behavior of S_1, S_2, V state variables for endemic case when $\tau_2 = 0.04$.

vaccination under different scenarios while varying the order of the fractional derivative. It is observed that an increase in vaccination rate and vaccine efficacy caused a reduction in the total number of new infections.

6. Conclusion

In this work, a novel fractional order mathematical model for the transmission dynamics of tuberculosis was designed and investigated. Uninfected vulnerable individuals are categorized into the following: susceptibles with underline ailment and susceptibles without underline ailment. The research seeks to qualitatively and quantitatively analyze the proposed model and suggests comprehensive intervention measures. The infection-free and endemic equilibria for the proposed model were also derived. Sensitivity analysis of the reproduction number was also assess the most dominant parameters influencing the dynamics of the disease within a given population. Specifically, the transmission rate, the vaccine efficacy, recovery and disease-induced death rates were the most influential parameters of the model.

It is recommended that to control TB within a population, efforts must be stepped up to encourage mass vaccination of individuals with underline ailments. The transmission of infection among individuals with comorbidity should also be reduced as much as possible. This study has limitations. Due to the unavailability of sufficient data, the study did not fit the model to real data. This is highly desired by the authors for further study. Also, future directions of our work shall investigate the use of more efficient numerical schemes, such as the non-standard finite difference scheme, for obtaining the solution. We also hope to investigate the impact of co-infection with other viral and bacterial diseases and how this can affect the control of TB.

Disclosure statement

No potential conflict of interest was reported by the author(s).

Notes on contributors

Dr. A. El-Mesady received the B.S. degree in industrial electronics and control engineering from Faculty of Electronic Engineering, Menoufia University, Egypt, in 2010, the M.S. degree in engineering mathematics from Faculty of Electronic Engineering, Menoufia university, Egypt, in 2014, and the Ph. D. degree in engineering mathematics from Faculty of Electronic Engineering, Menoufia University, Egypt, in 2018. He is currently an associate professor and a researcher in Faculty of Electronic Engineering, Menoufia University, Egypt. He is the author of many research articles published by Elsevier, Springer, MDPI, Charles Babbage Research Center, Taylor & Francis, Hindawi, IEEE, AIMS Press, IOP Publishing Ltd, and other well-known journals. His research interests include graph theory, combinatorial designs, and fractional calculus.

Dr. Olumuyiwa James Peter is a researcher in the Department Mathematical and Computer Sciences with a joint appointment to the Department of Epidemiology and Biostatistics, University of Medical Sciences, Ondo, Nigeria. He works in the area of Applied Mathematics. He was the immediate past Head of the Department of Mathematical and Computer Sciences and presently the Ag. Director, Center for Data Science and Health Metrics. His main research interests are in Biomathematics and Mathematical Modelling of Infectious Diseases. He is an author and co-author of several research papers in peer-reviewed journals locally and internationally in high impact journals. He is also a reviewer and editor of some of the top impact journals.

Dr. Andrew Omame is a lecturer at the Department of Mathematics, Federal University of Technology Owerri, Nigeria and currently a Postdoctoral Research Fellow at the Abdus Salam School of Mathematical Sciences Government College University Lahore Pakistan.

Dr. Festus Abiodun Oguntolu is a distinguished Senior Lecturer at the Federal University of Technology, Minna, Nigeria. His academic journey and research contributions have significantly advanced the fields of Mathematical Biology and Fractional Calculus. Known for his dedication to scientific inquiry and education, Dr. Oguntolu has been instrumental in developing and applying mathematical models to understand complex biological systems.

ORCID

Olumuyiwa James Peter http://orcid.org/0000-0001-9448-1164

References

[1] Pallett S, Houston A, Tuberculosis M. Medicine. 2021;49(12):751–755. doi: 10.1016/j.mpmed.2021.09.005

[2] Global tuberculosis report 2022. Geneva: World Health Organization; 2022. Licence: CC BY-NC-SA 3.0 IGO.

[3] Chakaya J, Khan M, Ntoumi F, et al. Global Tuberculosis Report 2020 - Reflections on the Global TB burden, treatment and prevention efforts. Inter J Infect Dis. 2021;113(1):S7–S12.

[4] Omame A, Abbas M. The stability analysis of a co-circulation model for COVID-19, dengue, and zika with nonlinear incidence rates and vaccination strategies. Healthcare Anal. 2023;3. doi: 10.1016/j.health.2023.100151.

[5] Omame A, Rwezaura H, Diagne ML, et al. COVID-19 and dengue co-infection in Brazil: optimal control and cost-effectiveness analysis. Eur Phys J Plus. 2021;136(10):1090.

[6] Omame A, Okuonghae D. A co-infection model for oncogenic human papillomavirus and tuberculosis

with optimal control and Cost-Effectiveness Analysis. Opt Contr Appl Meth. 2021;42(4):1081–1101.
[7] Diagne ML, Rwezaura H, Tchoumi SY, et al. A mathematical model of COVID-19 with vaccination and treatment. Compuy Math Med. 2021. doi: 10.1155/2021/1250129
[8] Chiyaka C, Garria W, Dube S. Modelling immune response and drug therapy in human malaria infection. Comput Math Methods Med. 2008;9(2):143–163.
[9] Idoko OB, Olumuyiwa James Peter WA, Bolaji B. Tawakalt Abosede Ayoola, A mathematical analysis of the two-strain tuberculosis model dynamics with exogenous re-infection. Healthcare Anal. 2023;100266. doi: 10.1016/j.health.2023.100266.
[10] James Peter O, Qureshi S, Yusuf A, et al. Abioye Abioye Idowu, A new mathematical model of COVID-19 using real data from Pakistan. Results Phys. 2021;24(104098). doi: 10.1016/j.rinp.2021.104098
[11] Ojo OB, Lougue S, Woldegerima WA. Bayesian generalized linear mixed modeling of Tuberculosis using informative priors. PLOS ONE. 2017;12(3):e0172580.
[12] Mohammed AO, Aatif A, Hussam A, et al. fractional order mathematical model for COVID-19 dynamics with quarantine, isolation, and environmental viral load. Adv Differ Equ. 2021;106. doi: 10.1186/s13662-021-03265-4.
[13] Nwankwo A, Okuonghae D. Mathematical Analysis of the Transmission Dynamics of HIV Syphilis Co-infection in the Presence of Treatment for Syphilis. Bull Math Biol. 2018;80(3):437–492.
[14] Abidemi A, Aziz NAB. Analysis of deterministic models for dengue disease transmission dynamics with vaccination perspective in Johor, Malaysia. Int J Appl Comput Math. 2022;8(45). doi: 10.1007/s40819-022-01250-3
[15] Sudhanshu KB, Uttam G, Susmita S, Mathematical model of zika virus dynamics with vector control and sensitivity analysis. Infect Dis Model. 2019 Dec 18;5:23–41. doi: 10.1016/j.idm.2019.12.001.eCollection2020
[16] Niger AM, Gumel AB. Immune response and imperfect vaccine in malaria dynamics. Math Popul Stud. 2011;18(2):55–86.
[17] Sene N. SIR epidemic model with Mittag-Leffler fractional derivative. Chaos Solitons Fract. 2020;137:109833.
[18] Tilahun GT, Woldegerima WA, Mohammed N. Getachew Teshome Tilahun, Woldegebriel Assefa Woldegerima & Nesredin Mohammed. A fractional order model for the transmission dynamics of hepatitis B virus with two-age structure in the presence of vaccination. Arab J Basic Appl Sci. 2021;28(1):87–106.
[19] Omame A, Isah ME, Abbas M, et al. A fractional order model for Dual Variants of COVID-19 and HIV co-infection via Atangana-Baleanu derivative. Alexandria Eng J. 2022;61(12):9715–9731. doi: 10.1016/j.aej.2022.03.013
[20] Rehman A, Singh R, Agarwal P. Modeling, analysis and prediction of new variants of covid-19 and dengue co-infection on complex network. Chaos Soliton Fract. 2021;150:111008.
[21] Peter OJ, Yusuf A, Oshinubi K, et al. Fractional order of pneumococcal pneumonia infection model with Caputo Fabrizio operator. Results Phys. 2021;29:104581.
[22] Peter OJ, Shaikh AS, Ibrahim MO, et al. Analysis and dynamics of fractional order mathematical model of COVID-19 in Nigeria using Atangana-Baleanu operator, Comput. Mater. Continua. 2021;1823–1848.
[23] O.j P. Transmission dynamics of fractional order brucellosis model using Caputo-Fabrizio operator. Int J Differ Equ Appl. 2020;2020.
[24] El-Mesady A, Adel W, Elsadany AA, et al. Stability analysis and optimal control strategies of a fractional-order Monkeypox virus infection model. Phys Scr. 2023;98(9):095256.
[25] Adel W, Amr Elsonbaty AA, El-Mesady A. Investigating the dynamics of a novel fractional-order monkeypox epidemic model with optimal control. Alexandria Eng J. 2023;73:519–542.
[26] El-Mesady A, Elsonbaty A, Adel W. On nonlinear dynamics of a fractional order monkeypox virus model. Chaos, Solitons Fractals. 2022;164:112716.
[27] Higazy M, El-Mesady A, Mahdy AMS, et al. Numerical, Approximate Solutions, and Optimal Control on the Deathly Lassa Hemorrhagic Fever Disease in Pregnant Women. J Funct Spaces. 2021;2021:1–15.
[28] Diethelm D, Ford NJ. Analysis of fractional differential equations. J Math Anal Appl. 2002;265(2):229–248.
[29] Ojo MM, Peter OJ, Goufo EFD, et al. Mathematical model for control of tuberculosis epidemiology. J Appl Math Comput. 2023;69(1):69–87.
[30] Ayinla AY, Othman WAM, Rabiu M. A Mathematical Model of the Tuberculosis Epidemic. Acta Biotheor. 2021;69(3):225–255.
[31] Ullah S, Altaf Khan M, Farooq M. Taza Gul, Modeling and analysis of Tuberculosis (TB) in Khyber Pakhtunkhwa, Pakistan. Math Comput Simul. 2019;165:181–199.
[32] Li Y, Chen Y, Podlubny I. Stability of fractional-order nonlinear dynamic systems: lyapunov direct method and generalized Mittag-Leffler stability. Comput Math Appl. 2010;59(5):1810–1821.
[33] Odibat ZM, Shawagfeh NT. Generalized taylors formula Appl. Math Comput. 2007;186:286–293.
[34] Tavazoei MS, Haeri M. Chaotic attractors in incommensurate fractional order systems. Physica D. 2008;237:2628–2637.
[35] Pontryagin LS. Mathematical theory of optimal processes. London, UK: Routledge; 2018.

Appendix A. Equation for finding R^{**}

$$
\begin{aligned}
&-\frac{\mu R\left(-\gamma_1\delta_1\omega+\gamma_1\delta_1+\gamma_2\delta_2+\gamma_1\mu+\gamma_2\mu+\gamma_1\gamma_2+\delta_1\mu+\delta_2\mu+\delta_1\delta_2+\mu^2\right)}{\gamma_1\gamma_2\theta}(\theta+\mu)+\frac{R\mu(1-\omega)\delta_1}{\gamma_2}\\
&+\frac{\mu\alpha_1\left(\mu+\gamma_2+\delta_1\right)\left(-\frac{\left(\frac{\rho\gamma_1\gamma_2\phi_1}{-R\alpha_1\mu^2-R\alpha_1\gamma_2\mu-\gamma_1\gamma_2\mu-R\alpha_1\delta_1\mu-\rho\gamma_1\gamma_2}+\frac{\rho\gamma_1\gamma_2\phi_2}{-R\alpha_2\mu^2-R\alpha_2\gamma_2\mu-\gamma_1\gamma_2\mu-R\alpha_2\delta_1\mu-\rho\gamma_1\gamma_2}\right)\tau_1}{-\frac{R(1-\varepsilon)\left(\alpha_1+\alpha_2\right)\left(\mu+\gamma_2+\delta_1\right)\mu}{\gamma_1\gamma_2}-\mu-\tau_1-\tau_2-\frac{\rho\gamma_1\gamma_2\tau_1}{-R\alpha_1\mu^2-R\alpha_1\gamma_2\mu-\gamma_1\gamma_2\mu-R\alpha_1\delta_1\mu-\rho\gamma_1\gamma_2}-\frac{\rho\gamma_1\gamma_2\tau_2}{-R\alpha_2\mu^2-R\alpha_2\gamma_2\mu-\gamma_1\gamma_2\mu-R\alpha_2\delta_1\mu-\rho\gamma_1\gamma_2}}-\phi_1\right)}{-R\alpha_1\mu^2-R\alpha_1\gamma_2\mu-\gamma_1\gamma_2\mu-R\alpha_1\delta_1\mu-\rho\gamma_1\gamma_2}\\
&+\frac{R\mu\alpha_2\left(\mu+\gamma_2+\delta_1\right)\left(-\frac{\left(\frac{\rho\gamma_1\gamma_2\phi_1}{-R\alpha_1\mu^2-R\alpha_1\gamma_2\mu-\gamma_1\gamma_2\mu-R\alpha_1\delta_1\mu-\rho\gamma_1\gamma_2}+\frac{\rho\gamma_1\gamma_2\phi_2}{-R\alpha_2\mu^2-R\alpha_2\gamma_2\mu-\gamma_1\gamma_2\mu-R\alpha_2\delta_1\mu-\rho\gamma_1\gamma_2}\right)\tau_2}{-\frac{R(1-\varepsilon)\left(\beta_1+\beta_2\right)\left(\mu+\gamma_2+\delta_1\right)\mu}{\gamma_1\gamma_2}-\mu-\tau_1-\tau_2-\frac{\rho\gamma_1\gamma_2\tau_1}{-R\alpha_1\mu^2-R\alpha_1\gamma_2\mu-\gamma_1\gamma_2\mu-R\alpha_1\delta_1\mu-\rho\gamma_1\gamma_2}-\frac{\rho\gamma_1\gamma_2\tau_2}{-R\alpha_2\mu^2-R\alpha_2\gamma_2\mu-\gamma_1\gamma_2\mu-R\alpha_2\delta_1\mu-\rho\gamma_1\gamma_2}}-\phi_2\right)}{-R\alpha_2\mu^2-R\alpha_2\gamma_2\mu-\gamma_1\gamma_2\mu-R\alpha_2\delta_1\mu-\rho\gamma_1\gamma_2}\\
&+\frac{R(1-\varepsilon)\mu(\alpha_1+\alpha_2)\left(\mu+\gamma_2+\delta_1\right)\left(\frac{\rho\gamma_1\gamma_2\phi_1}{-R\alpha_1\mu^2-R\alpha_1\gamma_2\mu-\gamma_1\gamma_2\mu-R\alpha_1\delta_1\mu-\rho\gamma_1\gamma_2}+\frac{\rho\gamma_1\gamma_2\phi_2}{-R\alpha_2\mu^2-R\alpha_2\gamma_2\mu-\gamma_1\gamma_2\mu-R\alpha_2\delta_1\mu-\rho\gamma_1\gamma_2}\right)}{\gamma_1\gamma_2\left(-\frac{R(1-\varepsilon)(\alpha_1+\alpha_2)\left(\mu+\gamma_2+\delta_1\right)\mu}{\gamma_1\gamma_2}-\mu-\tau_1-\tau_2-\frac{\rho\gamma_1\gamma_2\tau_1}{-R\alpha_1\mu^2-R\alpha_1\gamma_2\mu-\gamma_1\gamma_2\mu-R\alpha_1\delta_1\mu-\rho\gamma_1\gamma_2}-\frac{\rho\gamma_1\gamma_2\tau_2}{-R\alpha_2\mu^2-R\alpha_2\gamma_2\mu-\gamma_1\gamma_2\mu-R\alpha_2\delta_1\mu-\rho\gamma_1\gamma_2}\right)}=0.
\end{aligned}
$$

Appendix B. Sensitivity index

$$
S_{\phi_1}^{R_0}=\frac{\phi_1\left(\frac{\alpha_1(\tau_1(\mu+\rho)+\mu(\mu+\rho+\tau_2))}{\mu(\mu+\rho)(\mu+\rho+\tau_1+\tau_2)}+\frac{\alpha_2\rho\tau_2}{\mu(\mu+\rho)(\mu+\rho+\tau_1+\tau_2)}+\frac{\alpha_1\rho(1-\varepsilon)}{\mu(\mu+\rho+\tau_1+\tau_2)}+\frac{\alpha_2\rho(1-\varepsilon)}{\mu(\mu+\rho+\tau_1+\tau_2)}\right)}{\frac{\alpha_1(\phi_1(\tau_1(\mu+\rho)+\mu(\mu+\rho+\tau_2))+\rho\tau_1\phi_2)}{\mu(\mu+\rho)(\mu+\rho+\tau_1+\tau_2)}+\frac{\alpha_2(\mu\phi_2(\mu+\rho+\tau_1)+\tau_2(\phi_2(\mu+\rho)+\rho\phi_1))}{\mu(\mu+\rho)(\mu+\rho+\tau_1+\tau_2)}+\frac{\alpha_1\rho(1-\varepsilon)(\phi_1+\phi_2)}{\mu(\mu+\rho+\tau_1+\tau_2)}+\frac{\alpha_2\rho(1-\varepsilon)(\phi_1+\phi_2)}{\mu(\mu+\rho+\tau_1+\tau_2)}},
$$

$$
S_{\phi_2}^{R_0}=\frac{\phi_2\left(\frac{\alpha_1\rho\tau_1}{\mu(\mu+\rho)(\mu+\rho+\tau_1+\tau_2)}+\frac{\alpha_2(\mu(\mu+\rho+\tau_1)+\tau_2(\mu+\rho))}{\mu(\mu+\rho)(\mu+\rho+\tau_1+\tau_2)}+\frac{\alpha_1\rho(1-\varepsilon)}{\mu(\mu+\rho+\tau_1+\tau_2)}+\frac{\alpha_2\rho(1-\varepsilon)}{\mu(\mu+\rho+\tau_1+\tau_2)}\right)}{\frac{\alpha_1(\phi_1(\tau_1(\mu+\rho)+\mu(\mu+\rho+\tau_2))+\rho\tau_1\phi_2)}{\mu(\mu+\rho)(\mu+\rho+\tau_1+\tau_2)}+\frac{\alpha_2(\mu\phi_2(\mu+\rho+\tau_1)+\tau_2(\phi_2(\mu+\rho)+\rho\phi_1))}{\mu(\mu+\rho)(\mu+\rho+\tau_1+\tau_2)}+\frac{\alpha_1\rho(1-\varepsilon)(\phi_1+\phi_2)}{\mu(\mu+\rho+\tau_1+\tau_2)}+\frac{\alpha_2\rho(1-\varepsilon)(\phi_1+\phi_2)}{\mu(\mu+\rho+\tau_1+\tau_2)}},
$$

$$
S_{\alpha_1}^{R_0}=\frac{\alpha_1\left(\frac{\phi_1(\tau_1(\mu+\rho)+\mu(\mu+\rho+\tau_2))+\rho\tau_1\phi_2}{\mu(\mu+\rho)(\mu+\rho+\tau_1+\tau_2)}+\frac{\rho(1-\varepsilon)(\phi_1+\phi_2)}{\mu(\mu+\rho+\tau_1+\tau_2)}\right)}{\frac{\alpha_1(\phi_1(\tau_1(\mu+\rho)+\mu(\mu+\rho+\tau_2))+\rho\tau_1\phi_2)}{\mu(\mu+\rho)(\mu+\rho+\tau_1+\tau_2)}+\frac{\alpha_2(\mu\phi_2(\mu+\rho+\tau_1)+\tau_2(\phi_2(\mu+\rho)+\rho\phi_1))}{\mu(\mu+\rho)(\mu+\rho+\tau_1+\tau_2)}+\frac{\alpha_1\rho(1-\varepsilon)(\phi_1+\phi_2)}{\mu(\mu+\rho+\tau_1+\tau_2)}+\frac{\alpha_2\rho(1-\varepsilon)(\phi_1+\phi_2)}{\mu(\mu+\rho+\tau_1+\tau_2)}},
$$

$$
S_{\alpha_2}^{R_0}=\frac{\alpha_2\left(\frac{\mu\phi_2(\mu+\rho+\tau_1)+\tau_2(\phi_2(\mu+\rho)+\rho\phi_1)}{\mu(\mu+\rho)(\mu+\rho+\tau_1+\tau_2)}+\frac{\rho(1-\varepsilon)(\phi_1+\phi_2)}{\mu(\mu+\rho+\tau_1+\tau_2)}\right)}{\frac{\alpha_1(\phi_1(\tau_1(\mu+\rho)+\mu(\mu+\rho+\tau_2))+\rho\tau_1\phi_2)}{\mu(\mu+\rho)(\mu+\rho+\tau_1+\tau_2)}+\frac{\alpha_2(\mu\phi_2(\mu+\rho+\tau_1)+\tau_2(\phi_2(\mu+\rho)+\rho\phi_1))}{\mu(\mu+\rho)(\mu+\rho+\tau_1+\tau_2)}+\frac{\alpha_1\rho(1-\varepsilon)(\phi_1+\phi_2)}{\mu(\mu+\rho+\tau_1+\tau_2)}+\frac{\alpha_2\rho(1-\varepsilon)(\phi_1+\phi_2)}{\mu(\mu+\rho+\tau_1+\tau_2)}},
$$

$$S_{\rho}^{R_0}=\rho\Bigg(\frac{\alpha_1(\phi_1(\mu+\tau_1)+\tau_1\phi_2)}{\mu(\mu+\rho)(\mu+\rho+\tau_1+\tau_2)}+\frac{\alpha_2(\mu\phi_2+\tau_2(\phi_1+\phi_2))}{\mu(\mu+\rho)(\mu+\rho+\tau_1+\tau_2)}-\frac{\alpha_1(\phi_1(\tau_1(\mu+\rho)+\mu(\mu+\rho+\tau_2))+\rho\tau_1\phi_2)}{\mu(\mu+\rho)^2(\mu+\rho+\tau_1+\tau_2)}$$
$$-\frac{\alpha_2(\mu\phi_2(\mu+\rho+\tau_1)+\tau_2(\phi_2(\mu+\rho)+\rho\phi_1))}{\mu(\mu+\rho)^2(\mu+\rho+\tau_1+\tau_2)}-\frac{\alpha_1(\phi_1(\tau_1(\mu+\rho)+\mu(\mu+\rho+\tau_2))+\rho\tau_1\phi_2)}{\mu(\mu+\rho)(\mu+\rho+\tau_1+\tau_2)^2}$$
$$-\frac{\alpha_2(\mu\phi_2(\mu+\rho+\tau_1)+\tau_2(\phi_2(\mu+\rho)+\rho\phi_1))}{\mu(\mu+\rho)(\mu+\rho+\tau_1+\tau_2)^2}+\frac{\alpha_1(1-\varepsilon)(\phi_1+\phi_2)}{\mu(\mu+\rho+\tau_1+\tau_2)}+\frac{\alpha_2(1-\varepsilon)(\phi_1+\phi_2)}{\mu(\mu+\rho+\tau_1+\tau_2)}$$
$$-\frac{\alpha_1\rho(1-\varepsilon)(\phi_1+\phi_2)}{\mu(\mu+\rho+\tau_1+\tau_2)^2}-\frac{\alpha_2\rho(1-\varepsilon)(\phi_1+\phi_2)}{\mu(\mu+\rho+\tau_1+\tau_2)^2}\Bigg)/$$
$$\Bigg(\frac{\alpha_1(\phi_1(\tau_1(\mu+\rho)+\mu(\mu+\rho+\tau_2))+\rho\tau_1\phi_2)}{\mu(\mu+\rho)(\mu+\rho+\tau_1+\tau_2)}+\frac{\alpha_2(\mu\phi_2(\mu+\rho+\tau_1)+\tau_2(\phi_2(\mu+\rho)+\rho\phi_1))}{\mu(\mu+\rho)(\mu+\rho+\tau_1+\tau_2)}+$$
$$\frac{\alpha_1\rho(1-\varepsilon)(\phi_1+\phi_2)}{\mu(\mu+\rho+\tau_1+\tau_2)}+\frac{\alpha_2\rho(1-\varepsilon)(\phi_1+\phi_2)}{\mu(\mu+\rho+\tau_1+\tau_2)}\Bigg),$$

$$S_{\tau_1}^{R_0}=\tau_1\Bigg(\frac{\alpha_2\phi_2}{(\mu+\rho)(\mu+\rho+\tau_1+\tau_2)}+\frac{\alpha_1(\phi_1(\mu+\rho)+\rho\phi_2)}{\mu(\mu+\rho)(\mu+\rho+\tau_1+\tau_2)}-\frac{\alpha_1(\phi_1(\tau_1(\mu+\rho)+\mu(\mu+\rho+\tau_2))+\rho\tau_1\phi_2)}{\mu(\mu+\rho)(\mu+\rho+\tau_1+\tau_2)^2}$$
$$-\frac{\alpha_2(\mu\phi_2(\mu+\rho+\tau_1)+\tau_2(\phi_2(\mu+\rho)+\rho\phi_1))}{\mu(\mu+\rho)(\mu+\rho+\tau_1+\tau_2)^2}-\frac{\alpha_1\rho(1-\varepsilon)(\phi_1+\phi_2)}{\mu(\mu+\rho+\tau_1+\tau_2)^2}-\frac{\alpha_2\rho(1-\varepsilon)(\phi_1+\phi_2)}{\mu(\mu+\rho+\tau_1+\tau_2)^2}\Bigg)/$$
$$\Bigg(\frac{\alpha_1(\phi_1(\tau_1(\mu+\rho)+\mu(\mu+\rho+\tau_2))+\rho\tau_1\phi_2)}{\mu(\mu+\rho)(\mu+\rho+\tau_1+\tau_2)}+\frac{\alpha_2(\mu\phi_2(\mu+\rho+\tau_1)+\tau_2(\phi_2(\mu+\rho)+\rho\phi_1))}{\mu(\mu+\rho)(\mu+\rho+\tau_1+\tau_2)}$$
$$+\frac{\alpha_1\rho(1-\varepsilon)(\phi_1+\phi_2)}{\mu(\mu+\rho+\tau_1+\tau_2)}+\frac{\alpha_2\rho(1-\varepsilon)(\phi_1+\phi_2)}{\mu(\mu+\rho+\tau_1+\tau_2)}\Bigg),$$

$$S_{\tau_2}^{R_0}=\tau_2\Bigg(\frac{\alpha_1\phi_1}{(\mu+\rho)(\mu+\rho+\tau_1+\tau_2)}+\frac{\alpha_2(\phi_2(\mu+\rho)+\rho\phi_1)}{\mu(\mu+\rho)(\mu+\rho+\tau_1+\tau_2)}-\frac{\alpha_1(\phi_1(\tau_1(\mu+\rho)+\mu(\mu+\rho+\tau_2))+\rho\tau_1\phi_2)}{\mu(\mu+\rho)(\mu+\rho+\tau_1+\tau_2)^2}$$
$$-\frac{\alpha_2(\mu\phi_2(\mu+\rho+\tau_1)+\tau_2(\phi_2(\mu+\rho)+\rho\phi_1))}{\mu(\mu+\rho)(\mu+\rho+\tau_1+\tau_2)^2}-\frac{\alpha_1\rho(1-\varepsilon)(\phi_1+\phi_2)}{\mu(\mu+\rho+\tau_1+\tau_2)^2}-\frac{\alpha_2\rho(1-\varepsilon)(\phi_1+\phi_2)}{\mu(\mu+\rho+\tau_1+\tau_2)^2}\Bigg)/$$
$$\frac{\alpha_1(\phi_1(\tau_1(\mu+\rho)+\mu(\mu+\rho+\tau_2))+\rho\tau_1\phi_2)}{\mu(\mu+\rho)(\mu+\rho+\tau_1+\tau_2)}+\frac{\alpha_2(\mu\phi_2(\mu+\rho+\tau_1)+\tau_2(\phi_2(\mu+\rho)+\rho\phi_1))}{\mu(\mu+\rho)(\mu+\rho+\tau_1+\tau_2)}+$$
$$\frac{\alpha_1\rho(1-\varepsilon)(\phi_1+\phi_2)}{\mu(\mu+\rho+\tau_1+\tau_2)}+\frac{\alpha_2\rho(1-\varepsilon)(\phi_1+\phi_2)}{\mu(\mu+\rho+\tau_1+\tau_2)},$$

$$S_{\mu}^{R_0}=\mu(\theta+\mu)(\mu+\gamma_1+\delta_2)\Bigg(-\frac{\theta\Big(\frac{(1-\varepsilon)\rho\alpha_1(\phi_1+\phi_2)}{\mu(\mu+\rho+\tau_1+\tau_2)}+\frac{(1-\varepsilon)\rho\alpha_2(\phi_1+\phi_2)}{\mu(\mu+\rho+\tau_1+\tau_2)}+\frac{\alpha_1(((\mu+\rho)\tau_1+\mu(\mu+\rho+\tau_2))\phi_1+\rho\tau_1\phi_2)}{\mu(\mu+\rho)(\mu+\rho+\tau_1+\tau_2)}+\frac{\alpha_2(\mu(\mu+\rho+\tau_1)\phi_2+\tau_2(\rho\phi_1+(\mu+\rho)\phi_2))}{\mu(\mu+\rho)(\mu+\rho+\tau_1+\tau_2)}\Big)}{(\theta+\mu)^2(\mu+\gamma_1+\delta_2)}$$
$$-\frac{\theta\Big(\frac{(1-\varepsilon)\rho\alpha_1(\phi_1+\phi_2)}{\mu(\mu+\rho+\tau_1+\tau_2)}+\frac{(1-\varepsilon)\rho\alpha_2(\phi_1+\phi_2)}{\mu(\mu+\rho+\tau_1+\tau_2)}+\frac{\alpha_1(((\mu+\rho)\tau_1+\mu(\mu+\rho+\tau_2))\phi_1+\rho\tau_1\phi_2)}{\mu(\mu+\rho)(\mu+\rho+\tau_1+\tau_2)}+\frac{\alpha_2(\mu(\mu+\rho+\tau_1)\phi_2+\tau_2(\rho\phi_1+(\mu+\rho)\phi_2))}{\mu(\mu+\rho)(\mu+\rho+\tau_1+\tau_2)}\Big)}{(\theta+\mu)(\mu+\gamma_1+\delta_2)^2}$$
$$+\theta\Bigg(\frac{\alpha_1(2\mu+\rho+\tau_1+\tau_2)\phi_1}{\mu(\mu+\rho)(\mu+\rho+\tau_1+\tau_2)}+\frac{\alpha_2(\mu\phi_2+(\mu+\rho+\tau_1)\phi_2+\tau_2\phi_2)}{\mu(\mu+\rho)(\mu+\rho+\tau_1+\tau_2)}-\frac{(1-\varepsilon)\rho\alpha_1(\phi_1+\phi_2)}{\mu^2(\mu+\rho+\tau_1+\tau_2)}-$$
$$\frac{(1-\varepsilon)\rho\alpha_2(\phi_1+\phi_2)}{\mu^2(\mu+\rho+\tau_1+\tau_2)}-\frac{\alpha_1(((\mu+\rho)\tau_1+\mu(\mu+\rho+\tau_2))\phi_1+\rho\tau_1\phi_2)}{\mu^2(\mu+\rho)(\mu+\rho+\tau_1+\tau_2)}$$
$$-\frac{\alpha_2(\mu(\mu+\rho+\tau_1)\phi_2+\tau_2(\rho\phi_1+(\mu+\rho)\phi_2))}{\mu^2(\mu+\rho)(\mu+\rho+\tau_1+\tau_2)}-\frac{\alpha_1(((\mu+\rho)\tau_1+\mu(\mu+\rho+\tau_2))\phi_1+\rho\tau_1\phi_2)}{\mu(\mu+\rho)^2(\mu+\rho+\tau_1+\tau_2)}-$$
$$\frac{\alpha_2(\mu(\mu+\rho+\tau_1)\phi_2+\tau_2(\rho\phi_1+(\mu+\rho)\phi_2))}{\mu(\mu+\rho)^2(\mu+\rho+\tau_1+\tau_2)}-\frac{(1-\varepsilon)\rho\alpha_1(\phi_1+\phi_2)}{\mu(\mu+\rho+\tau_1+\tau_2)^2}$$
$$-\frac{(1-\varepsilon)\rho\alpha_2(\phi_1+\phi_2)}{\mu(\mu+\rho+\tau_1+\tau_2)^2}-\frac{\alpha_1(((\mu+\rho)\tau_1+\mu(\mu+\rho+\tau_2))\phi_1+\rho\tau_1\phi_2)}{\mu(\mu+\rho)(\mu+\rho+\tau_1+\tau_2)^2}-\frac{\alpha_2(\mu(\mu+\rho+\tau_1)\phi_2+\tau_2(\rho\phi_1+(\mu+\rho)\phi_2))}{\mu(\mu+\rho)(\mu+\rho+\tau_1+\tau_2)^2}\Bigg)(\theta+\mu)(\mu+\gamma_1+\delta_2)$$

$$/\theta\Bigg(\frac{(1-\varepsilon)\rho\alpha_1(\phi_1+\phi_2)}{\mu(\mu+\rho+\tau_1+\tau_2)}+\frac{(1-\varepsilon)\rho\alpha_2(\phi_1+\phi_2)}{\mu(\mu+\rho+\tau_1+\tau_2)}+\frac{\alpha_1(((\mu+\rho)\tau_1+\mu(\mu+\rho+\tau_2))\phi_1+\rho\tau_1\phi_2)}{\mu(\mu+\rho)(\mu+\rho+\tau_1+\tau_2)}$$
$$+\frac{\alpha_2(\mu(\mu+\rho+\tau_1)\phi_2+\tau_2(\rho\phi_1+(\mu+\rho)\phi_2))}{\mu(\mu+\rho)(\mu+\rho+\tau_1+\tau_2}\Bigg)$$

$$S_{\varepsilon}^{R_0}=\frac{\varepsilon\left(-\frac{\alpha_1\rho(\phi_1+\phi_2)}{\mu(\mu+\rho+\tau_1+\tau_2)}-\frac{\alpha_2\rho(\phi_1+\phi_2)}{\mu(\mu+\rho+\tau_1+\tau_2)}\right)}{\frac{\alpha_1(\phi_1(\tau_1(\mu+\rho)+\mu(\mu+\rho+\tau_2))+\rho\tau_1\phi_2)}{\mu(\mu+\rho)(\mu+\rho+\tau_1+\tau_2)}+\frac{\alpha_2(\mu\phi_2(\mu+\rho+\tau_1)+\tau_2(\phi_2(\mu+\rho)+\rho\phi_1))}{\mu(\mu+\rho)(\mu+\rho+\tau_1+\tau_2)}+\frac{\alpha_1\rho(1-\varepsilon)(\phi_1+\phi_2)}{\mu(\mu+\rho+\tau_1+\tau_2)}+\frac{\alpha_2\rho(1-\varepsilon)(\phi_1+\phi_2)}{\mu(\mu+\rho+\tau_1+\tau_2)}},$$

$$S_{\delta_1}^{R_0}=0,\ S_{\delta_2}^{R_0}=-\frac{\delta_2}{\gamma_1+\delta_2+\mu},\ S_{\gamma_1}^{R_0}=-\frac{\gamma_1}{\gamma_1+\delta_2+\mu},\ S_{\gamma_2}^{R_0}=0,\ S_{\omega}^{R_0}=0,$$

$$S_{\theta}^{R_0}=(\theta+\mu)(\gamma_1+\delta_2+\mu)\Bigg(\frac{\frac{\alpha_1(\phi_1(\tau_1(\mu+\rho)+\mu(\mu+\rho+\tau_2))+\rho\tau_1\phi_2)}{\mu(\mu+\rho)(\mu+\rho+\tau_1+\tau_2)}+\frac{\alpha_2(\mu\phi_2(\mu+\rho+\tau_1)+\tau_2(\phi_2(\mu+\rho)+\rho\phi_1))}{\mu(\mu+\rho)(\mu+\rho+\tau_1+\tau_2)}+\frac{\alpha_1\rho(1-\varepsilon)(\phi_1+\phi_2)}{\mu(\mu+\rho+\tau_1+\tau_2)}+\frac{\alpha_2\rho(1-\varepsilon)(\phi_1+\phi_2)}{\mu(\mu+\rho+\tau_1+\tau_2)}}{(\theta+\mu)(\gamma_1+\delta_2+\mu)}$$
$$-\frac{\theta(\frac{\alpha_1(\phi_1(\tau_1(\mu+\rho)+\mu(\mu+\rho+\tau_2))+\rho\tau_1\phi_2)}{\mu(\mu+\rho)(\mu+\rho+\tau_1+\tau_2)}+\frac{\alpha_2(\mu\phi_2(\mu+\rho+\tau_1)+\tau_2(\phi_2(\mu+\rho)+\rho\phi_1))}{\mu(\mu+\rho)(\mu+\rho+\tau_1+\tau_2)}+\frac{\alpha_1\rho(1-\varepsilon)(\phi_1+\phi_2)}{\mu(\mu+\rho+\tau_1+\tau_2)}+\frac{\alpha_2\rho(1-\varepsilon)(\phi_1+\phi_2)}{\mu(\mu+\rho+\tau_1+\tau_2)})}{(\theta+\mu)^2(\gamma_1+\delta_2+\mu)}\Bigg)$$
$$\Bigg(/\frac{\alpha_1(\phi_1(\tau_1(\mu+\rho)+\mu(\mu+\rho+\tau_2))+\rho\tau_1\phi_2)}{\mu(\mu+\rho)(\mu+\rho+\tau_1+\tau_2)}+\frac{\alpha_2(\mu\phi_2(\mu+\rho+\tau_1)+\tau_2(\phi_2(\mu+\rho)+\rho\phi_1))}{\mu(\mu+\rho)(\mu+\rho+\tau_1+\tau_2)}$$
$$+\frac{\alpha_1\rho(1-\varepsilon)(\phi_1+\phi_2)}{\mu(\mu+\rho+\tau_1+\tau_2)}+\frac{\alpha_2\rho(1-\varepsilon)(\phi_1+\phi_2)}{\mu(\mu+\rho+\tau_1+\tau_2)}\Bigg)$$